Phage-mediated resolution of genetic conflict alters the evolutionary trajectory of *Pseudomonas aeruginosa* lysogens

Authors: Laura C. Suttenfield[1,2], Zoi Rapti[2,3], Jayadevi H. Chandrashekhar[2], Amelia C. Steinlein[1,2], Juan Cristobal Vera[2], Ted Kim[1,2], Rachel J. Whitaker[1,2*]

1. Department of Microbiology, School of Molecular and Cellular Biology, University of Illinois at Urbana-Champaign, Urbana, Illinois
2. Carl R. Woese Institute for Genomic Biology, University of Illinois at Urbana-Champaign, Urbana, Illinois
3. Department of Mathematics, University of Illinois at Urbana-Champaign, Urbana, Illinois

*Correspondence: rwhitakr@illinois.edu

Abstract

The opportunistic human pathogen *Pseudomonas aeruginosa* is naturally infected by a large class of temperate, transposable, Mu-like phages. We examined the genotypic and phenotypic diversity of *P. aeruginosa* PA14 populations as they resolve CRISPR autoimmunity, mediated by an imperfect CRISPR match to the Mu-like phage DMS3 prophage, and show that lysogen evolution is profoundly impacted by CRISPR autoimmunity and phage transposition around the chromosome. After 12 days of evolution, we measured a decrease in spontaneous induction in both exponential and stationary phase growth. Co-existing variation in spontaneous induction rates in exponential phase corresponded to a difference in the mutational modes of CRISPR self-targeting resolution, mediated either by host mutation or phage transposition. Multiple mutational modes to resolve genetic conflict between host and phage resulted in coexistence in evolved populations of single lysogens that maintained immunity to other phages and polylysogens that have lost immunity completely. This work provides more insight into the nature of viral evolution in single ancestor lysogen populations like the CF lung, and highlights a new dimension to the role of lysogenic phages on the evolution of their hosts.

Importance

The chronic opportunistic multi-drug resistant pathogen *Pseudomonas aeruginosa* is persistently infected by temperate phages. We assess the contribution of temperate phage infection to the evolution of the clinically relevant strain UCBPP-PA14. We found that a low level of CRISPR-mediated self-targeting resulted in polylysogeny evolution and large genome rearrangements in lysogens; we also found extensive diversification in CRISPR spacers and *cas* genes. These genomic modifications resulted in decreased spontaneous induction in both exponential and stationary phase growth, increasing lysogen fitness. This work shows the importance of considering latent phage infection in characterizing the evolution of bacterial populations.

Keywords: lysogen; spontaneous induction; evolution; CRISPR; transposable phages

Introduction

Cystic fibrosis (CF) is a genetic disorder which makes patients vulnerable to respiratory infections by commensal and environmental bacterial pathogens like *Pseudomonas aeruginosa*. *Pseudomonas aeruginosa* is a common human pathogen whose increase in multi-drug antibiotic resistance has made it the focus of targeted phage therapy (Kortright et al., 2019). In chronic *Pseudomonas* infections of CF patients, it is common to find that all isolates track their origin to a single ancestral genotype (Feliziani et al., 2014; Folkesson et al., 2012; Jorth et al., 2015; Markussen et al., 2014; Schick & Kassen, 2018; Tai et al., 2017; Workentine et al., 2013). Diversity of *P. aeruginosa* strains diverge from this common ancestor through *de novo* mutations generated by mutation and hypermutation genotypes (Vanderwoude et al., 2023), recombination (Darch et al., 2015; Vanderwoude et al., 2023) and large deletions (Cramer et al., 2011; Jeukens et al., 2014; Rau et al., 2012).

Pseudomonas aeruginosa is commonly infected by latent phages (bacteriophage) when colonizing CF patients (Budzik et al., 2004; Burgener et al., 2019; Folkesson et al., 2012; Ojeniyi et al., 1991; Rossi et al., 2021; Tariq et al., 2019; Vanderwoude et al., 2023; Winstanley et al., 2016). Temperate and chronic phages act as both sources of genetic novelty (Brüssow et al., 2004) and as potential assassins that can be induced to kill their hosts (James et al., 2015; Willner et al., 2012). In the lung environment, the presence of antibiotics and reactive oxygen species (Kettle et al., 2014; Malhotra et al., 2019; McGrath et al., 1999) may act as inducing agents for phage (Bondy-Denomy et al., 2016; Fothergill et al., 2011; James et al., 2015; Nanda et al., 2015; Rolain et al., 2009). Bacterial lysis through phage induction is hypothesized to help control bacterial growth in the lung (James et al., 2015) and may be used in synergy with antibiotics (Al-Anany et al., 2021; Clifton et al., 2019). Additionally, lysogeny has been shown to co-occur with host genome rearrangements in chronically infecting *Staphylococcus aureus* (Goerke et al., 2004, 2006; Golubchik et al., 2013; Guérillot et al., 2019), and *Streptococcus pyogenes* (Nakagawa et al., 2003). However, it remains unclear if and how lysogeny alters the evolution of the host genome.

Mu-like transposable phages are a diverse family of phages which infect an equally diverse range of bacteria (Zhang et al., 2023). Upon infection of the host, Mu-like phages integrate into the host chromosome through a conservative (cut-and-paste) transposition step that occurs with low sequence preference (Chaconas & Harshey, 2007; Vergnaud et al., 2018; Walker et al., 2020). Lytic replication occurs via replicative (copy-and-paste) transposition around the genome (Walker & Harshey, 2020), which occurs approximately 100 times and terminates in headful packaging into the virion. In lysogeny, which is established in approximately 10% of infections, a low-specificity insertion can increase the variation available to natural selection in *P. aeruginosa* populations through knockout mutations (Davies et al., 2016; O'Brien et al., 2019; Rollie et al., 2020). These *P. aeruginosa* lysogens have previously been found to have high viral titers in culture (Bondy-Denomy et al., 2016; James et al., 2012). Due to the nature of the chemistry that governs the transposition reaction, these insertions may also cause structural rearrangements such as deletions (Toussaint & Rice, 2017).

78 CRISPR-Cas (clustered regularly interspaced short palindromic repeats and CRISPR-associated genes) is a
79 bacterial and archaeal adaptive immune system which incorporates foreign DNA fragments into an array as a
80 spacer, and subsequently targets any piece of invading DNA (the protospacer) which is complementary to the
81 spacer (Barrangou et al., 2007; Vorontsova et al., 2015). The Mu-like temperate phage are the most
82 commonly targeted phages by CRISPR-Cas in *Pseudomonas aeruginosa* (England et al., 2018). Phage
83 DMS3, a member of this group, was recovered from a *P. aeruginosa* CF isolate and infects the type strain
84 UCBPP-PA14 (Budzik et al., 2004). DMS3 inhibits quorum sensing and pilus formation in PA14 lysogens
85 (Shah et al., 2021). PA14 contains a Type 1-F CRISPR system with a partial spacer match to DMS3 (Zegans
86 et al., 2009). This spacer has 5 mismatches to the phage protospacer, which is not sufficient to mediate
87 immunity to the phage but leads to genetic conflict in DMS3 lysogens. This degenerate protospacer-spacer
88 mismatch between DMS3 and PA14 targets the PA14 chromosome, ultimately leading to a biofilm formation
89 defect (Heussler et al., 2015). In an engineered phage-free system with only the phage protospacer in the
90 PA14 genome, the presence of the phage protospacer alone causes enough DNA damage to stimulate the
91 SOS response, which leads to the expression of pyocin genes, cell death, and limitation of biofilm formation
92 (Heussler et al., 2015). Lysogens arising from PA14 cultures infected with free DMS3 virions evolved to have
93 a lower spontaneous induction in stationary phase and lost their CRISPR systems over a seven-day
94 evolutionary period. This was suggested to resolve genetic conflict between CRISPR self-targeting
95 (immunopathology) and phage induction (Rollie et al., 2020). However, the mechanism of genotype loss and
96 evolution of the DMS3 lysogen has not yet been explored.
97
98 Here we directly assess the contribution of CRISPR-mediated genetic conflict between host and temperate
99 phage to the evolution of *Pseudomonas* by analyzing evolved lysogen populations. We show that selection to
100 resolve genetic conflict alters the evolutionary landscape of lysogen populations. Experimental work combined
101 with genomic analysis demonstrates that transposable phages are a major source of variation beyond mutation
102 that impacts the evolutionary direction of *P. aeruginosa* lysogens.
103
104

105 ## Methods

106 **Experimental evolution**

107 To establish the contribution of phages to host genome evolution, we evolved the established lysogen Lys2
108 (Zegans et al., 2009) for 12 days by serial transfer. Our strains are listed in Table S1. Lys2 is derived from
109 PA14 and contains DMS3, which mediated a ~20 kb host deletion from 806,169 to 826,108 bp on our PA14
110 reference chromosome, and a single A<G nonsynonymous point mutation at position 4,755,306 in a
111 hypothetical protein (deleted genes are listed in Table S2). For each strain we randomly selected three
112 colonies and grew up independent overnight cultures in LB (10 g tryptone; 5 g yeast extract; 5 g sodium
113 chloride per liter of water). We subcultured the cells and normalized to an OD_{600} of 0.2 in 25 mL microcosms in
114 three parallel 250 mL flasks. We serially passaged triplicate cultures with daily 1:100 transfers for 12 days,
115 with shaking and at 37°C, for approximately 72 bacterial generations. At the end of the experiment, we colony-

purified six colonies isolated from each replicate, and six colonies from the Lys2 ancestor stock for further analysis.

One-step growth curves

In order to calculate the burst size of DMS3, we performed one-step growth curves (Ellis & Delbrück, 1939). Overnight, stationary phase PA14 cultures were diluted 1:100 and grown in LB until they reached an OD of 0.5. Phage was added to these cultures at a 1:10 volume ratio, for a final MOI of 0.01, mixed well, and incubated at 37°C for 5 minutes. In order to calculate adsorption, a fraction of the sample volume was immediately spun down for 5 mins at 30,000 rpm, and the supernatant was stored with 10% v/v chloroform to quantify the remaining free phage. To begin the one-step growth curve, the remainder of the samples were added to pre-warmed medium at a 1:100 ratio to stop adsorption, and grown on a roller drum at 37°C for the next 2.5 hours. Samples were taken every 10 minutes and mixed with a 10% v/v of chloroform for later quantification of PFUs.

We calculated burst size with the following equation: the total phage produced (the difference between the average PFUs before and after the burst) was divided by number of cells that were infected (estimated by the number of adsorbed phages multiplied by the estimated number of cells which proceeded through lysis). Our measurements of an 8% lysogenization frequency, estimated by spot-on-lawn assay, corresponded to measures in (Cady & O'Toole, 2011) (data not shown).

$$\beta = \frac{p_2 - p_1}{c_i * (1 - l)}$$

Here, β is burst size; p_2 and p_1 are the second and first plateaus, respectively; c_i is the number of infected cells; l is the lysogenization frequency. The burst size of DMS3 is 41.8 +/- 8.4 phages per lysed cell (Fig S1). All PFUs were enumerated by spotting the phage-containing fraction on 0.5% double agar overlay plates.

Spontaneous induction measurements

Growth curves were started from overnight cultures of replicate purified isolates. We washed cultures three times by resuspension in fresh LB media, normalized the OD to 0.2, and diluted them 1000-fold. Time points were taken at 0 and 2-7 hours to capture exponential phase growth, and plated for both CFUs and PFUs. Samples were incubated at 37°C on a roller drum. We measured spontaneous induction (q) by taking the difference in the number of viral particles released by cells growing in exponential phase, and normalized by the estimated burst size, the average growth of the culture, and the total time the culture grew.

$$q = \frac{\Delta V}{(\beta * \Delta t * C)}$$

Here, q is spontaneous induction, and has units of burst cells per time; ΔV is the total increase in virion particles; β is the burst size; Δt is the change in time; C is the average amount of cells in the culture. To

account for exponential growth, all calculations were based on the linear regression of the $\log_{10}$ transformed ΔV and C values.

We also calculated spontaneous induction based on calculations in (Zong et al., 2010). This paper approximated spontaneous induction at each time point with this formula: $q = \frac{V}{\beta C}$; here, V is the number of virion particles at that time; β is the burst size; and C is the average amount of CFUs at that time. These methods produced qualitatively similar results (Fig S2).

To measure induction in stationary phase, we began growth curves in the same way as the exponential phase measurements. Time points were taken at 0, 10, 12, 15, and 18 hours, and plated for both CFUs and PFUs. To calculate the rate of spontaneous induction, we used the same formula as above, except with un-regressed logged values.

Genome sequencing

In order to create a viral reference, DMS3 DNA was extracted from filtered Lys2 overnight supernatant using the Phage DNA Isolation Kit (Norgen Biotek Corp, Cat #: 46800), following the manufacturer's instructions. Libraries were prepared with a Biomek 4000 liquid handler (Beckman-Coulter). We quantitated libraries with a Qubit fluorometer (Life Technologies Corporation, REF #: Q32866). Libraries were pooled and submitted for 2x250 paired-end sequencing by the Roy J. Carver Biotechnology Center at the University of Illinois Urbana-Champaign with an Illumina NovaSeq 6000. We received ~3.8 million reads with about 100X coverage.

We inoculated evolved isolates and ancestral controls in 2 mL deep well plates in LB and grew them overnight. We extracted gDNA with the Beckman-Coulter gDNA extraction kit as above using the Nextera Flex Library Preparation Kit (Illumina). We quantitated libraries with a Qubit fluorometer (Life Technologies Corporation, REF #: Q32866). Libraries were pooled and submitted for 2x250 paired-end sequencing by the Roy J. Carver Biotechnology Center at the University of Illinois Urbana-Champaign with an Illumina NovaSeq 6000. We received an average of about 5 million reads per genome. All raw reads are available on the NCBI database under BioProject number PRJNA1021667.

Genome analysis

We ran a custom QC pipeline on our raw FASTQ reads, available on Github (http://www.github.com/igoh-illinois). Briefly, the Illumina adaptor sequences were trimmed using TrimmomaticPE v0. Read quality was checked with FastQC v0.11.9 (options: --noextract -k 5 -f fastq). Reads were aligned using BWA-MEM (Li, 2013) with default options to a 2-contig reference genome containing both our reference PA14 sequence and our reference DMS3 sequence. To identify chromosomal mutations, we ran Breseq (Deatherage & Barrick, 2014) on the trimmed and quality-controlled reads. SAM files were checked manually in both IGV 2.12.3 (J. T. Robinson et al., 2017) and Tablet (Milne et al., 2013).

To identify insertion sites of transposable phage, we ran a second pipeline, available on Github (http://www.github.com/igoh-illinois). The pipeline identifies insertion sites at nucleotide resolution by identifying split reads that map to both the host and viral chromosome. It further identifies insertion sites by finding reads that have been split on either side of a 5-bp window, creating a small overlapping region when mapped back to the host genome. This is the result of a 5-bp duplication, which is characteristic of Mu and Mu-like phage transposition (Allet, 1979; Morgan et al., 2002).

While manually verifying the phage insertion sites in IGV, we found putative large duplicated regions of the host chromosome. To verify these duplicated regions we used the depth command in Samtools (Danecek et al., 2021) to find the number of reads that covered each position in the genome, and graphed this using RStudio (R version 4.3.1) (R Core Team, 2023). In order to assess the protein content of deleted and duplicated regions, FASTA files of sequence the reference PA14 genome was given to the eggNOG-mapper-v2 pipeline (settings: genomic data; default options) (Cantalapiedra et al., 2021).

Mitomycin C induction experiments

Single colonies of the strains of interest were inoculated in LB, grown overnight at 37°C on a roller drum, and subcultured until they reached an OD of 0.5. Cultures were normalized, split, and incubated with or without 0.5 µg/µL mitomycin C (MMC) for 3.5 hours, after which CFUs and PFUs were enumerated.

Model information

We use a compartmental model based on a system of ordinary differential equations. There are six lysogen compartments each representing a lysogen characterized by a distinct rate of spontaneous induction, but otherwise being identical. Lysogens are induced at their associated rates and transition into the lytic state which is followed by phage production and bursting. The model is along the lines of the ones presented and analyzed in our previous works (Clifton et al., 2019, 2021; Landa et al., 2021). All lysogens are assumed to grow at the same rate, and the total bacterial population grows logistically. The model equations read:

$$\frac{dL_i}{dt} = rL_i\left(1 - \sum_{j=1}^{6}\left(L_j + I_j\right)\right) - q_iL_i$$

$$\frac{dI_i}{dt} = -\delta I_i + q_iL_i$$

$$\frac{dV_i}{dt} = \beta\delta I_i - \mu V_i$$

We have partially non-dimensionalized the model so that 1 time unit in the simulations corresponds to about 50 minutes. The lysogeny growth rate is denoted by r, the spontaneous induction rates by $q_i, i = 1, \ldots, 6$, the rate of phage production by δ, the burst size is by β, and the rate of viral degradation by μ. The first two equations

are decoupled from the last one describing the phage (since we do not consider superinfections in this model). Therefore, the dynamics of the bacterial compartments resemble those of generalized Lotka-Volterra competition.

Statistical measures

Data visualization and statistical analyses were performed in R version 4.3.1 (R Core Team, 2023) using the packages tidyverse version 2.0.0 (Wickham et al., 2019), car version 3.1-2 (Fox & Weisberg, 2019), rstatix version 0.7.2, and emmeans version 1.8.6.

Results

Evolution of a self-targeting lysogen results in decreased spontaneous induction in exponential and stationary phase.

After 12 days and ~72 generations of exponential growth in rich media, we found that the spontaneous induction of DMS3 lysogens was significantly reduced compared to ancestral isolates in exponential phase (Fig 1; ANOVA, $F_{3,68} = 16.7$, $P < 1e\text{-}8$). Isolate induction rates within and between experimental replicates ranged from 0.1% to 0.71% of the culture, while the induction rates of ancestral PA14 lysogen (Lys2) isolates ranged from 0.38% to 1.1% of the culture (Fig 1A). Significant differences were robust to the use of other metrics to estimate spontaneous induction (Zong et al., 2010) (see Figure S3). Spontaneous induction was also significantly decreased in stationary phase for all evolved lysogens (Fig S3; ANOVA, $F_{3,109} = 86.98$, $P < 2.2e\text{-}16$), although compared to exponential phase, induction was very reduced in stationary phase overall, indicating that the majority of spontaneous induction takes place in exponential phase in DMS3 lysogens.

Lysogen populations maintain diversity in CRISPR presence and function.

Sequencing of lysogens from each population showed that lysogens evolved the CRISPR locus through a combination of mutation and large deletions and other structural variants (Table 1, Fig 2). 39% (7/18) of isolates mutated or deleted the mismatched spacer in the CRISPR2 array, which contains the mismatched spacer which targets the integrated DMS3 (Fig 2B, Fig S4). Two mutations occurred in parallel between two different replicate populations in the evolved lysogen treatment: an A to G point mutation in the seed region of the self-targeting spacer, and an exact deletion of the self-targeting spacer and its upstream repeat (Fig 2B). 22% (4/18) of isolates had disruptions (three independent frameshift mutations and a small deletion) within the *cas* genes *cas7* and *cas8* which form part of the complex that mediates interference in *P. aeruginosa* (Chowdhury et al., 2017). Of these three frameshift mutations, one led to the predicted loss of the *cas7* RNA-binding domain, and two are predicted to interfere with the cas3-recruitment or interaction domain of cas8 (Fig 2B, Table 1). One strain was recovered with a 3 kb deletion in the *cas* gene region that spans *cas5* (also part

262 of the interference complex) and *cas7*. While each strain with mutations and indels in the CRISPR array likely
263 no longer target the DMS3 prophage, they maintain CRISPR function.
264
265 We observed that 44% (8/18) of evolved lysogen isolates carried deletions of varying sizes; the smallest being
266 the 3 kb deletion in the *cas* genes, and the largest deletion, 335,331 bp, comprising about 5% of the PA14
267 chromosome. Of these eight deletions, seven were centered on the CRISPR2 array (Fig 2C). Therefore, in
268 the evolved lysogen populations, we observed extensive coexistence between combinations of CRISPR
269 spacer mutations and large entire deletions of CRISPR caused by phage transposition, demonstrating the
270 importance of phage infection in determining distinct evolutionary trajectories in isolates in the same
271 environment.
272
273 **Evolved lysogens with large deletions are polylysogens.**
274 While confirming that the evolved lysogens had retained the phage at its original integration site (Methods), we
275 found that the boundaries of the deletions of the CRISPR2 array were composed of reads that mapped to both
276 the PA14 and DMS3 chromosomes (hereafter referred to as "split" reads), indicating that the large deletions in
277 these seven isolates resulted from a DMS3 transposition event which occurred from within the chromosome
278 (Fig 3). These phage-mediated deletions ranged from approximately 34-335 kb (mean = 163.3 kb ± 100.3 kb).
279 Deletions occurred in each of the replicates independently, with no shared deletion boundaries even within the
280 same culture (Fig 2C). The regions of the phage chromosome to which the split reads mapped and the
281 orientation of phage reads at the boundaries of the deletions in two samples (1_4 and 2_3) suggests that more
282 than one phage genome may be inserted in the gap (Table 2).
283
284 The large deletions, though centered around the CRISPR locus, had different deletion boundaries. To assess
285 the shared gene content in these regions, we used eggNOG-mapper to query the functional protein content
286 (Methods). In addition to CRISPR, the deleted regions were enriched with genes from COG category S (genes
287 of unknown function), which included Type 6 secretion system-related genes *tssF* and *tssG* , and multiple
288 pyoverdine system genes which are often lost during lung colonization (Nguyen et al., 2014; O'Brien et al.,
289 2017; Schick & Kassen, 2018). Several pyoverdine biosynthesis and transport genes (*fpvA, pvdE, pvdH, pvdI,*
290 *pvdM, pvdM, pvdO*) were deleted in 6 of the 7 isolates with large deletions. *PvdS,* a regulator of pyoverdine
291 biosynthesis genes (Leoni et al., 2000), and *pvdR,* a component of the pyoverdine efflux transporter (Imperi et
292 al., 2009), were also deleted in 5 of the 7 isolates with large deletions. The co-localization of these virulence
293 and defense gene cassettes with CRISPR may contribute to variation in these regions (Makarova et al., 2011;
294 L. A. Robinson et al., 2023).
295
296 In this study, 100% (7/7) of isolates with large deletions were polylysogens; however, polylysogeny did not
297 evolve in cells that resolved self-targeting via CRISPR mutations from SNPs or indels (Fig S7). Similarly, a
298 previous study showed that PA14, when challenged with free DMS3 virions and subjected to a short-term
299 evolution experiment, evolved genome deletions encompassing the CRISPR region when the susceptible host

300 did not have self-targeting (e.g. contained a *cas7* deletion) (see: Extended Data Table 1 in Rollie *et al*, 2020).
301 In combination with our data, we infer that self-targeting increases the rate of DMS3 transposition, resulting in
302 polylysogens, which then are maintained in the population only when they are associated with adaptive
303 mutations, such as those which decrease spontaneous induction by resolving genetic conflict (Fig S7; for
304 model, see Fig 6).
305
306 **Evolved polylysogens contain large duplications.**
307 Three isolates containing phage-mediated large deletions in CRISPR also had large duplications elsewhere in
308 the genome (27, 188, and 244 kb; mean = 153 ± 113 kb) that were bounded by viral insertion sites. In these
309 cases, these regions were not deleted but were doubled in coverage (Fig 3, Fig S5A, S5B). Due to the
310 orientation of the PA14/DMS3 split reads at these insertion sites, which faced away from each other rather
311 than toward each other, and due to the fact that the split reads at the boundaries of the duplicated regions only
312 represented about 50% of the total coverage, we interpret these regions to be large duplications with a phage
313 genome in the middle, as opposed to two independent viral insertions (Fig S5C). As the duplicated regions
314 were not centered around a shared core, they were almost completely non-overlapping in their gene content.
315 Only one known gene was duplicated in two of the three isolates (Lys2_ev_pop2_3 and Lys2_ev_pop2_6),
316 which was *betT,* a choline transporter known to accumulate mutations in clinical isolates from CF patients
317 (Malek et al., 2011; Marvig et al., 2015; Stribling et al., 2023). Broadly, genes from category H (coenzyme
318 metabolism) were represented in all three isolates, as well as from P (inorganic ion metabolism) and S (genes
319 of unknown function), as in the large deletions. Several genes annotated as part of the major facilitator
320 superfamily, a class of membrane-associated transporter proteins, were also duplicated in two of the three
321 isolates, as well as genes from the *moa* family, which have recently been implicated in biofilm formation
322 (Kaleta & Sauer, 2023).
323
324 Two of these duplications (in 1_4 and 2_6) independently evolved a shared boundary six nucleotides apart (at
325 positions 1120309 and 1120303, respectively), in an intergenic region between the 3' end of a hypothetical
326 protein and the 3' end of an AraC transcriptional regulator. An analysis of all new lysogen insertion sites
327 (including the deletion and duplication boundaries) using the motif-finding software MEME Suite did not return
328 any motifs, either using MEME (searching for a motif in a 15 bp region centered on the insertion site), or
329 MEME-ChIP (searching for centrally enriched motifs 250 bp around the insertion site) (Bailey & Elkan, 1994;
330 Machanick & Bailey, 2011); this suggests parallel duplications may be advantageous in this environment.
331
332 Neither the isolates containing large deletions nor the ones containing large duplications differed in their growth
333 from other evolved strains that did not have large structural variation (Fig S6A). This suggests that, under
334 these conditions, the fitness costs to deletions, duplications or carrying additional copies of the phage in the
335 chromosome are smaller than the fitness gains by removing self-targeting. Although these phage-mediated
336 deletions of CRISPR represent the addition of one to two phage genomes to the lysogen chromosome, the
337 spontaneous induction rate of these isolates remains reduced relative to the ancestral PA14 lysogen strain

338 (Lys2) (Fig 1, Fig S6B). Additionally, although viral output does not change with phage genome copy number
339 after challenge with mitomycin C, cell survival is significantly increased with increased phage genomes (Fig
340 S6C), suggesting a possible mechanism of viral interference leading to cell survival which may also contribute
341 to a decreased spontaneous induction measurement.
342
343 **Spontaneous induction correlates with mutation.**
344 We observed that spontaneous induction was variable within replicate populations (Fig 1). We asked whether
345 this variation might correlate with difference in the type of CRISPR mutation (SNP, deletions, viral
346 transpositions) by grouping lysogens into 1 of 5 categories based on the type of mutation that occurred in that
347 genome: “cas deletion”; “cas mutation”; “spacer deletion”; “spacer mutation”; and “large deletion polylysogen”.
348 We observed that all groups (with the exception of the cas deletion group, which had only one isolate in its
349 group) had significantly lower spontaneous induction than the ancestral strains (Fig 4); and the large deletion
350 polylysogen group was significantly lower than lysogens that had lowered spontaneous induction via SNPs or
351 indels. A model incorporating mutation type was a significantly better fit than the model by experimental
352 replicate (ANOVA, $F_{2,66}$ = 13.777, P < 1e-6). We find that heterogeneity in genotype correlates to the
353 heterogeneity in phenotype of spontaneous induction in our evolved lysogens.
354
355 Given these small but significant variations in spontaneous induction that are maintained within groups yet
356 replaced the ancestral lysogen genotype, we wanted to understand how long the diversity we observed within
357 our experimental replicates could persist in exponentially growing cultures. To do this, we developed a
358 mathematical model to compare six lysogens with six different rates of spontaneous induction (two values from
359 the ancestral group, two values from the host-mutation group, two values from the large deletion polylysogen
360 group). In a deterministic model of lysogen growth in exponential phase with varied spontaneous induction
361 rates, we founded populations with low densities of high inducers (representing the ancestor strain) and
362 allowed them to grow for 10 hours. At that time, we introduced either strains with low rates of spontaneous
363 induction (representing the large deletions) or medium rates of spontaneous induction (representing host
364 mutations), one at 10 hours and the other at 24 hours, and tested whether they could invade. We found that
365 when low inducers are introduced to a high-inducing population, medium inducers cannot subsequently invade
366 (Fig 5A). When we introduced medium inducers to a high-inducer population after 10 hours of growth, and
367 then low inducers after 24 hours, medium and low inducers outcompeted the high inducers and then coexisted
368 in the absence of the high inducers for about two days (Fig 5B). This coexistence recapitulates the observed
369 recovery of low and medium inducers, but not high inducers, in our experimental data (Fig 4). From these
370 observations we find that the weak selection imposed by these small differences in spontaneous induction,
371 which are caused by different mutational mechanisms, combined with the order in which they were introduced,
372 may allow evolution of diversity in CRISPR self-targeting resolution in *P. aeruginosa* lysogens and preserve
373 coexistence of CRISPR+ and CRISPR- strains in the absence of additional selective variables or
374 environmental change.
375

Discussion

Although temperate phages are frequently recovered from long-term, evolving *Pseudomonas* infections of the lungs of CF patients, phages are often considered at single time points or outside of relationship to their bacterial hosts (Ambroa et al., 2020; Gabrielaite et al., 2020; Tariq et al., 2015, 2019). Evolution experiments involving transposable phages often include susceptible cells, or are begun with free phages instead of established lysogens (Davies et al., 2016; Marshall et al., 2021; O'Brien et al., 2019; Rollie et al., 2020). Here, we query the impact of a phage on the evolution of its host genome in the context of established lysogeny, and find that the presence of temperate phage alone causes infected cells to follow an evolutionary trajectory in an island-like environment.

Our work supports previous studies showing that DMS3 lysogens evolve decreased rates of spontaneous induction over time; we distinguish between exponential and stationary phase, and find that exponential phase induction accounts for the majority of induced phages. Our spontaneous induction estimates in exponential phase are approximately 0.37% and 0.72% of the evolved and ancestral populations, respectively, which are both significantly higher than lambda-like phages (Imamovic et al., 2016; Little et al., 1999; Zong et al., 2010), but are in line with other studies that report high spontaneous induction (Owen et al., 2017). Mu-like phages have been reported previously to naturally produce high titers during lysogen growth (Bondy-Denomy et al., 2016; James et al., 2012; Zegans et al., 2009), suggesting that Mu-like phages as a family have high spontaneous induction rates and that this evolutionary pressure is not restricted to DMS3. We find that these high titers in overnight culture are not due to additional induction in stationary phase, as the rates of induction in stationary phase were much lower than in exponential phase even in wildtype lysogens. Because Mu-like phages are both highly prevalent and highly targeted (England et al., 2018), it is likely that CRISPR self-targeting will inform evolutionary outcomes in these related phages. Here, the resolution of that self-targeting resulted in coexisting variation in lysogen spontaneous induction rates in exponential growth, with polylysogens having the lowest rates perhaps due to viral interference preventing or slowing cell death, and lowering virion production.

We find that the genetic conflict between Mu-like phage and host results in a tradeoff between CRISPR immunity and spontaneous induction. Half of the evolved lysogen isolates decreased their spontaneous induction while maintaining either CRISPR function (in mutations or deletions of the self-targeting spacer) or the potential of CRISPR function (frameshift mutations in *cas* genes), while the rest deleted CRISPR and lost any potential immunity, but more substantially decreased their induction. One explanation for the maintenance of these two genotypes is the order in which these mutations were introduced. Modeling simulations show that spontaneous induction rates from strains which resolved self-targeting via SNPs and indels ("medium" inducers) cannot invade established populations of strains with spontaneous induction rates from polylysogens. This indicates that host-mediated SNPs and indels likely arose before polylysogeny and large deletions, as both are maintained together despite spontaneous induction differences. This suggestion of an order (host-mediated before phage-mediated) then suggests that the basal rate of phage transposition is lower

than host mutation. A lower rate of formation of higher-fitness polylysogen “low” inducers, which compete with lower-fitness host-mutation “medium” inducers with a faster rate of formation, may work to maintain a pool of diversity that selection may subsequently act on in different ways, given the presence of other phages or other ecological factors (Watson et al., 2023).

In an isolated environment, our model predicts that diversity would likely be resolved by the eventual replacement of CRISPR-immune cells with non-immune polylysogens, thereby increasing the phage copy number in an environment that does not have new susceptible hosts for horizontal transmission (Weitz et al., 2019). However, complex communities with additional phage and bacteria may then select for cells which maintain CRISPR function but which have higher spontaneous induction (Alseth et al., 2019; Gloag et al., 2019). How phages evolve increased fitness while maintaining CRISPR immunity and defense against other phages and bacterial competitors in complex environments remains an open question.

The results of genetic conflict in evolved lysogens are not limited to CRISPR deletions and may impact the rate of evolution of bacteria with latent infections. Gene loss and genome reduction have also been shown to occur in *P. aeruginosa* lineages during adaptation to the human lung, although the contribution of phages is unclear (Gabrielaite et al., 2020; Rau et al., 2012). In our study, pyoverdine and Type 6 secretion system genes were lost in the majority of the polylysogens; these genes are often lost in chronic CF isolates (Marvig et al., 2015; O’Brien et al., 2017; Perault et al., 2020). Whether and how phage presence continues to alter the evolution of its host from the uninfected state, and how phage infection influences the rate and mechanism of this evolution, are questions which require future study to explain the ubiquity of phage infection in many clinical environments (Burgener et al., 2019; Holloway et al., 1960; Vaca-Pacheco et al., 1999).

P. aeruginosa evolution in the context of the CF lung can occur via a slow accumulation of SNPs and indels (Marvig et al., 2015) or a more rapid accumulation of SNPs due to the evolution of hypermutator genotypes (Marvig et al., 2015; Oliver et al., 2000). Lysogenization by transposable phages offers a different mechanism of within-lung diversification which operates in addition to the baseline mutation rate. Future studies should aim to assess the functional role that deletions and duplications have on CF lung-specific phenotypes. The dependence of transposition on the presence of self-targeting, and by extension on low levels of DNA damage, also opens the possibility of other causes of low levels of DNA damage – for example, subinhibitory concentrations of DNA-damaging antibiotics – to be driving evolutionary adaptation and diversity in bacteria lysogenized by transposable phages. The extent to which phage infection informs differences in evolutionary and functional outcomes in a clinical context is an important subject for future work.

Acknowledgements

We are grateful to George O’Toole for discussions as well as strains of bacteria and phages described herein including Lys2, the ΔR/F pyocin operon strain, and DMS3. We gratefully acknowledge Dr. Alan Collins for

helpful discussions during early stages of this project. We thank Whitaker lab members Jiayue Yang for helpful discussions, and Sierra Bedwell and Izzy Lakis for comments on the manuscript. We thank Alvaro Hernandez and Chris Wright of the Roy J. Carver Biotechnology Institute for sequencing expertise, as well as Jeff Haas of the School of Integrative Biology for crucial help with data storage and server access. This work is funded by grants from the Cystic Fibrosis Foundation and the Allen Distinguished Investigator Award from the Paul G. Allen Foundation to R.J.W. and the National Science Foundation grant DMS-1815764 to Z.R. This research is also a contribution of the GEMS Biology Integration Institute, funded by the National Science Foundation DBI Integration Institutes Program, Award #2022049.

Author Contributions

Conceptualization: L.C.S., R.J.W. Formal analysis: L.C.S. Funding acquisition: L.C.S., R.J.W. Investigation: L.C.S., Z.R., A.C.S. Methodology: L.C.S., Z.R., J.H.C., R.J.W. Resources: J.C.V., R.J.W. Software: J.C.V. Visualization: L.C.S., Z.R. Writing – original draft: L.C.S., R.J.W. Writing – review and editing: L.C.S., R.J.W.

466

Group	Sample ID	Mutated region	Description	Due to phage	Location on PA14-REF chromosome
ev_pop1	ev_pop1_1	CRISPR2 sp1-8	Deletion	No	2936222-2936676
ev_pop1	ev_pop1_1	*tssK*	Nonsynonymous	No	94370
ev_pop1	ev_pop1_2	CRISPR2 sp1-4	Deletion	No	2936462-2936675
ev_pop1	ev_pop1_3	Δ 243,737 bp	Includes CRISPR region	Yes	2835111-3078848
ev_pop1	ev_pop1_4	Δ 186,866 bp	Includes CRISPR region	Yes	2839227-3026093
ev_pop1	ev_pop1_4	27,769 bp	Duplicated region	Yes	1120309-1148078
ev_pop1	ev_pop1_4	*cysT*	$(CAG)_{4\rightarrow3}$	No	329528
ev_pop1	ev_pop1_5	CRISPR2 sp1	A<G mutation in the 2nd nt	No	2936674
ev_pop1	ev_pop1_6	CRISPR2 sp1	GAT<G deletion of 1st and 2nd nt	No	2936673
ev_pop2	ev_pop2_1	Δ 88,123 bp	Includes CRISPR region	Yes	2921860
ev_pop2	ev_pop2_2	*cas8*	Frameshift (predicted loss of C-term helical bundle region)	No	2929846
ev_pop2	ev_pop2_3	Δ 194,512 bp	Includes CRISPR region	Yes	2890191-3084703
ev_pop2	ev_pop2_3	187,901 bp	Duplicated region	Yes	6222744-6410645
ev_pop2	ev_pop2_4	CRISPR2 sp1	Deletion	No	2936643-2936675
ev_pop2	ev_pop2_5	CRISPR2 sp1	A<G mutation in the 2nd nt	No	2936674
ev_pop2	ev_pop2_6	Δ 335,331 bp	Includes CRISPR region	Yes	2811042-3146373
ev_pop2	ev_pop2_6	244,019 bp	Duplicated region	Yes	876284-1120303
ev_pop2	ev_pop2_6	Intergenic region	$(GCCAAC)_{11\rightarrow8}$	No	3792568
ev_pop3	ev_pop3_1	*cas8*	Frameshift (retention of first 57/435 aa)	No	2930725
ev_pop3	ev_pop3_2	CRISPR2 sp1	Deletion	No	2936644-2936675
ev_pop3	ev_pop3_3	*cas7*	Frameshift (predicted loss of RNA-binding domain)	No	2927776
ev_pop3	ev_pop3_4	Δ 60,538 bp	Begins in *cas3* gene and includes CRISPR2 array	Yes	2934007-2994541
ev_pop3	ev_pop3_5	Δ 34,249 bp	Includes CRISPR region	Yes	2903549-2937794
ev_pop3	ev_pop3_6	Cas gene deletion	Deletion of *cas7* and *cas5*, partial deletion of *cas6* and *cas8*	No	2927288-2930093

467 **Table 1. Description of mutations recovered in evolved lysogens.**

468

Sample ID	Group	Upstream deletion boundary Read mate maps to:	Downstream deletion boundary Read mate maps to:
Lys2_ev_pop1_3	ev_pop_1	end of DMS3 genome	start of DMS3 genome
***Lys2_ev_pop1_4**	ev_pop_1	start of DMS3 genome	start of DMS3 genome
Lys2_ev_pop2_1	ev_pop_2	end of DMS3 genome	start of DMS3 genome
***Lys2_ev_pop2_3**	ev_pop_2	start of DMS3 genome	start of DMS3 genome
Lys2_ev_pop2_6	ev_pop_2	end of DMS3 genome	start of DMS3 genome
Lys2_ev_pop3_4	ev_pop_3	end of DMS3 genome	start of DMS3 genome
Lys2_ev_pop3_5	ev_pop_3	end of DMS3 genome	start of DMS3 genome

Table 2. Origin of phage reads at the deletion boundaries. Asterisks denote samples where reads from only one end of the phage genome were recovered.

472 ## References

473 Al-Anany, A. M., Fatima, R., & Hynes, A. P. (2021). Temperate phage-antibiotic synergy eradicates bacteria
474 through depletion of lysogens. *Cell Reports*, *35*(8), 109172.
475 https://doi.org/10.1016/j.celrep.2021.109172

476 Allet, B. (1979). Mu insertion duplicates a 5 base pair sequence at the host inserted site. *Cell*, *16*(1), 123–129.
477 https://doi.org/10.1016/0092-8674(79)90193-4

478 Alseth, E. O., Pursey, E., Luján, A. M., McLeod, I., Rollie, C., & Westra, E. R. (2019). Bacterial biodiversity drives
479 the evolution of CRISPR-based phage resistance. *Nature*, *574*(7779), 549–552.
480 https://doi.org/10.1038/s41586-019-1662-9

481 Ambroa, A., Blasco, L., López-Causapé, C., Trastoy, R., Fernandez-García, L., Bleriot, I., Ponce-Alonso, M.,
482 Pacios, O., López, M., Cantón, R., Kidd, T. J., Bou, G., Oliver, A., & Tomás, M. (2020). Temperate
483 Bacteriophages (Prophages) in Pseudomonas aeruginosa Isolates Belonging to the International Cystic
484 Fibrosis Clone (CC274). *Frontiers in Microbiology*, *11*, 556706.
485 https://doi.org/10.3389/fmicb.2020.556706

486 Bailey, T. L., & Elkan, C. (1994). Fitting a mixture model by expectation maximization to discover motifs in
487 biopolymers. *Proceedings. International Conference on Intelligent Systems for Molecular Biology*, *2*, 28–
488 36.

489 Barrangou, R., Fremaux, C., Deveau, H., Richards, M., Boyaval, P., Moineau, S., Romero, D. A., & Horvath, P.
490 (2007). CRISPR Provides Acquired Resistance Against Viruses in Prokaryotes. *Science*, *315*(5819), 1709–
491 1712. https://doi.org/10.1126/science.1138140

492 Bondy-Denomy, J., Qian, J., Westra, E. R., Buckling, A., Guttman, D. S., Davidson, A. R., & Maxwell, K. L. (2016).
493 Prophages mediate defense against phage infection through diverse mechanisms. *The ISME Journal*,
494 *10*(12), 2854–2866. https://doi.org/10.1038/ismej.2016.79

495 Brüssow, H., Canchaya, C., & Hardt, W.-D. (2004). Phages and the Evolution of Bacterial Pathogens: From
496 Genomic Rearrangements to Lysogenic Conversion. *Microbiology and Molecular Biology Reviews*,
497 *68*(3), 560–602. https://doi.org/10.1128/MMBR.68.3.560-602.2004
498 Budzik, J. M., Rosche, W. A., Rietsch, A., & O'Toole, G. A. (2004). Isolation and Characterization of a
499 Generalized Transducing Phage for Pseudomonas aeruginosa Strains PAO1 and PA14. *Journal of*
500 *Bacteriology*, *186*(10), 3270–3273. https://doi.org/10.1128/JB.186.10.3270-3273.2004
501 Burgener, E. B., Sweere, J. M., Bach, M. S., Secor, P. R., Haddock, N., Jennings, L. K., Marvig, R. L., Johansen, H.
502 K., Rossi, E., Cao, X., Tian, L., Nedelec, L., Molin, S., Bollyky, P. L., & Milla, C. E. (2019). Filamentous
503 bacteriophages are associated with chronic Pseudomonas lung infections and antibiotic resistance in
504 cystic fibrosis. *Science Translational Medicine*, *11*(488), eaau9748.
505 https://doi.org/10.1126/scitranslmed.aau9748
506 Cady, K. C., & O'Toole, G. A. (2011). Non-Identity-Mediated CRISPR-Bacteriophage Interaction Mediated via
507 the Csy and Cas3 Proteins. *Journal of Bacteriology*, *193*(14), 3433–3445.
508 https://doi.org/10.1128/JB.01411-10
509 Cantalapiedra, C. P., Hernández-Plaza, A., Letunic, I., Bork, P., & Huerta-Cepas, J. (2021). *eggNOG-mapper v2:*
510 *Functional Annotation, Orthology Assignments, and Domain Prediction at the Metagenomic Scale*
511 [Preprint]. Bioinformatics. https://doi.org/10.1101/2021.06.03.446934
512 Chaconas, G., & Harshey, R. M. (2007). Transposition of Phage Mu DNA. In N. L. Craig, R. Craigie, M. Gellert, &
513 A. M. Lambowitz (Eds.), *Mobile DNA II* (1st ed., pp. 384–402). Wiley.
514 https://doi.org/10.1128/9781555817954.ch17
515 Chowdhury, S., Carter, J., Rollins, M. F., Golden, S. M., Jackson, R. N., Hoffmann, C., Nosaka, L., Bondy-Denomy,
516 J., Maxwell, K. L., Davidson, A. R., Fischer, E. R., Lander, G. C., & Wiedenheft, B. (2017). Structure
517 Reveals Mechanisms of Viral Suppressors that Intercept a CRISPR RNA-Guided Surveillance Complex.
518 *Cell*, *169*(1), 47-57.e11. https://doi.org/10.1016/j.cell.2017.03.012

519 Clifton, S. M., Kim, T., Chandrashekhar, J. H., O'Toole, G. A., Rapti, Z., & Whitaker, R. J. (2019). Lying in Wait:
520 Modeling the Control of Bacterial Infections via Antibiotic-Induced Proviruses. *mSystems*, *4*(5).
521 https://doi.org/10.1128/mSystems.00221-19
522 Clifton, S. M., Whitaker, R. J., & Rapti, Z. (2021). Temperate and chronic virus competition leads to low lysogen
523 frequency. *Journal of Theoretical Biology*, *523*, 110710. https://doi.org/10.1016/j.jtbi.2021.110710
524 Cramer, N., Klockgether, J., Wrasman, K., Schmidt, M., Davenport, C. F., & Tümmler, B. (2011). Microevolution
525 of the major common Pseudomonas aeruginosa clones C and PA14 in cystic fibrosis lungs: P.
526 aeruginosa microevolution in cystic fibrosis. *Environmental Microbiology*, *13*(7), 1690–1704.
527 https://doi.org/10.1111/j.1462-2920.2011.02483.x
528 Danecek, P., Bonfield, J. K., Liddle, J., Marshall, J., Ohan, V., Pollard, M. O., Whitwham, A., Keane, T., McCarthy,
529 S. A., Davies, R. M., & Li, H. (2021). Twelve years of SAMtools and BCFtools. *GigaScience*, *10*(2),
530 giab008. https://doi.org/10.1093/gigascience/giab008
531 Darch, S. E., McNally, A., Harrison, F., Corander, J., Barr, H. L., Paszkiewicz, K., Holden, S., Fogarty, A., Crusz, S.
532 A., & Diggle, S. P. (2015). Recombination is a key driver of genomic and phenotypic diversity in a
533 Pseudomonas aeruginosa population during cystic fibrosis infection. *Scientific Reports*, *5*(1), Article 1.
534 https://doi.org/10.1038/srep07649
535 Davies, E. V., James, C. E., Williams, D., O'Brien, S., Fothergill, J. L., Haldenby, S., Paterson, S., Winstanley, C., &
536 Brockhurst, M. A. (2016). Temperate phages both mediate and drive adaptive evolution in pathogen
537 biofilms. *Proceedings of the National Academy of Sciences*, *113*(29), 8266–8271.
538 https://doi.org/10.1073/pnas.1520056113
539 Deatherage, D. E., & Barrick, J. E. (2014). Identification of mutations in laboratory evolved microbes from next-
540 generation sequencing data using breseq. *Methods in Molecular Biology (Clifton, N.J.)*, *1151*, 165–188.
541 https://doi.org/10.1007/978-1-4939-0554-6_12
542 Ellis, E. L., & Delbrück, M. (1939). The Growth of Bacteriophage. *The Journal of General Physiology*, *22*(3), 365–
543 384. https://doi.org/10.1085/jgp.22.3.365

544 England, W. E., Kim, T., & Whitaker, R. J. (2018). Metapopulation Structure of CRISPR-Cas Immunity in
545 Pseudomonas aeruginosa and Its Viruses. *mSystems*, *3*(5), e00075-18.
546 https://doi.org/10.1128/mSystems.00075-18
547 Feliziani, S., Marvig, R. L., Luján, A. M., Moyano, A. J., Rienzo, J. A. D., Johansen, H. K., Molin, S., & Smania, A.
548 M. (2014). Coexistence and Within-Host Evolution of Diversified Lineages of Hypermutable
549 Pseudomonas aeruginosa in Long-term Cystic Fibrosis Infections. *PLOS Genetics*, *10*(10), e1004651.
550 https://doi.org/10.1371/journal.pgen.1004651
551 Folkesson, A., Jelsbak, L., Yang, L., Johansen, H. K., Ciofu, O., Høiby, N., & Molin, S. (2012). Adaptation of
552 Pseudomonas aeruginosa to the cystic fibrosis airway: An evolutionary perspective. *Nature Reviews*
553 *Microbiology*, *10*(12), 841–851. https://doi.org/10.1038/nrmicro2907
554 Fothergill, J. L., Mowat, E., Walshaw, M. J., Ledson, M. J., James, C. E., & Winstanley, C. (2011). Effect of
555 Antibiotic Treatment on Bacteriophage Production by a Cystic Fibrosis Epidemic Strain of Pseudomonas
556 aeruginosa. *Antimicrobial Agents and Chemotherapy*, *55*(1), 426–428.
557 https://doi.org/10.1128/AAC.01257-10
558 Fox, J., & Weisberg, S. (2019). *An R Companion to Applied Regression*. Sage Publications.
559 https://socialsciences.mcmaster.ca/jfox/Books/Companion
560 Gabrielaite, M., Johansen, H. K., Molin, S., Nielsen, F. C., & Marvig, R. L. (2020). Gene Loss and Acquisition in
561 Lineages of Pseudomonas aeruginosa Evolving in Cystic Fibrosis Patient Airways. *mBio*, *11*(5), e02359-
562 20. https://doi.org/10.1128/mBio.02359-20
563 Gloag, E. S., Marshall, C. W., Snyder, D., Lewin, G. R., Harris, J. S., Santos-Lopez, A., Chaney, S. B., Whiteley, M.,
564 Cooper, V. S., & Wozniak, D. J. (2019). Pseudomonas aeruginosa Interstrain Dynamics and Selection of
565 Hyperbiofilm Mutants during a Chronic Infection. *mBio*, *10*(4), e01698-19.
566 https://doi.org/10.1128/mBio.01698-19
567 Goerke, C., Matias y Papenberg, S., Dasbach, S., Dietz, K., Ziebach, R., Kahl, B. C., & Wolz, C. (2004). Increased
568 Frequency of Genomic Alterations in *Staphylococcus aureus* during Chronic Infection Is in Part Due to

569 Phage Mobilization. *The Journal of Infectious Diseases*, *189*(4), 724–734.
570 https://doi.org/10.1086/381502
571 Goerke, C., Wirtz, C., Fluckiger, U., & Wolz, C. (2006). Extensive phage dynamics in Staphylococcus aureus
572 contributes to adaptation to the human host during infection. *Molecular Microbiology*, *61*(6), 1673–
573 1685. https://doi.org/10.1111/j.1365-2958.2006.05354.x
574 Golubchik, T., Batty, E. M., Miller, R. R., Farr, H., Young, B. C., Larner-Svensson, H., Fung, R., Godwin, H., Knox,
575 K., Votintseva, A., Everitt, R. G., Street, T., Cule, M., Ip, C. L. C., Didelot, X., Peto, T. E. A., Harding, R. M.,
576 Wilson, D. J., Crook, D. W., & Bowden, R. (2013). Within-Host Evolution of Staphylococcus aureus
577 during Asymptomatic Carriage. *PLoS ONE*, *8*(5), e61319. https://doi.org/10.1371/journal.pone.0061319
578 Guérillot, R., Kostoulias, X., Donovan, L., Li, L., Carter, G. P., Hachani, A., Vandelannoote, K., Giulieri, S., Monk,
579 I. R., Kunimoto, M., Starrs, L., Burgio, G., Seemann, T., Peleg, A. Y., Stinear, T. P., & Howden, B. P.
580 (2019). Unstable chromosome rearrangements in *Staphylococcus aureus* cause phenotype switching
581 associated with persistent infections. *Proceedings of the National Academy of Sciences*, *116*(40),
582 20135–20140. https://doi.org/10.1073/pnas.1904861116
583 Heussler, G. E., Cady, K. C., Koeppen, K., Bhuju, S., Stanton, B. A., & O'Toole, G. A. (2015). Clustered Regularly
584 Interspaced Short Palindromic Repeat-Dependent, Biofilm-Specific Death of Pseudomonas aeruginosa
585 Mediated by Increased Expression of Phage-Related Genes. *mBio*, *6*(3), e00129-15.
586 https://doi.org/10.1128/mBio.00129-15
587 Holloway, B. W., Egan, J. B., & Monk, M. (1960). Lysogeny in Pseudomonas Aeruginosa. *Australian Journal of*
588 *Experimental Biology and Medical Science*, *38*(4), 321–330. https://doi.org/10.1038/icb.1960.34
589 Imamovic, L., Ballesté, E., Martínez-Castillo, A., García-Aljaro, C., & Muniesa, M. (2016). Heterogeneity in
590 phage induction enables the survival of the lysogenic population. *Environmental Microbiology*, *18*(3),
591 957–969. https://doi.org/10.1111/1462-2920.13151

592 Imperi, F., Tiburzi, F., & Visca, P. (2009). Molecular basis of pyoverdine siderophore recycling in Pseudomonas
593 aeruginosa. *Proceedings of the National Academy of Sciences*, *106*(48), 20440–20445.
594 https://doi.org/10.1073/pnas.0908760106
595 James, C. E., Davies, E. V., Fothergill, J. L., Walshaw, M. J., Beale, C. M., Brockhurst, M. A., & Winstanley, C.
596 (2015). Lytic activity by temperate phages of Pseudomonas aeruginosa in long-term cystic fibrosis
597 chronic lung infections. *The ISME Journal*, *9*(6), Article 6. https://doi.org/10.1038/ismej.2014.223
598 James, C. E., Fothergill, J. L., Kalwij, H., Hall, A. J., Cottell, J., Brockhurst, M. A., & Winstanley, C. (2012).
599 Differential infection properties of three inducible prophages from an epidemic strain of Pseudomonas
600 aeruginosa. *BMC Microbiology*, *12*(1), 216. https://doi.org/10.1186/1471-2180-12-216
601 Jeukens, J., Boyle, B., Kukavica-Ibrulj, I., Ouellet, M. M., Aaron, S. D., Charette, S. J., Fothergill, J. L., Tucker, N.
602 P., Winstanley, C., & Levesque, R. C. (2014). Comparative Genomics of Isolates of a Pseudomonas
603 aeruginosa Epidemic Strain Associated with Chronic Lung Infections of Cystic Fibrosis Patients. *PLoS*
604 *ONE*, *9*(2), e87611. https://doi.org/10.1371/journal.pone.0087611
605 Jorth, P., Staudinger, B. J., Wu, X., Hisert, K. B., Hayden, H., Garudathri, J., Harding, C. L., Radey, M. C., Rezayat,
606 A., Bautista, G., Berrington, W. R., Goddard, A. F., Zheng, C., Angermeyer, A., Brittnacher, M. J.,
607 Kitzman, J., Shendure, J., Fligner, C. L., Mittler, J., … Singh, P. K. (2015). Regional Isolation Drives
608 Bacterial Diversification within Cystic Fibrosis Lungs. *Cell Host & Microbe*, *18*(3), 307–319.
609 https://doi.org/10.1016/j.chom.2015.07.006
610 Kaleta, M. F., & Sauer, K. (2023). MoaB1 Homologs Contribute to Biofilm Formation and Motility by
611 Pseudomonas aeruginosa and Escherichia coli. *Journal of Bacteriology*, *205*(5), e00004-23.
612 https://doi.org/10.1128/jb.00004-23
613 Kettle, A. J., Turner, R., Gangell, C. L., Harwood, D. T., Khalilova, I. S., Chapman, A. L., Winterbourn, C. C., Sly, P.
614 D., & on behalf of AREST CF. (2014). Oxidation contributes to low glutathione in the airways of children
615 with cystic fibrosis. *European Respiratory Journal*, *44*(1), 122–129.
616 https://doi.org/10.1183/09031936.00170213

617 Kortright, K. E., Chan, B. K., Koff, J. L., & Turner, P. E. (2019). Phage Therapy: A Renewed Approach to Combat
618 Antibiotic-Resistant Bacteria. *Cell Host & Microbe*, *25*(2), 219–232.
619 https://doi.org/10.1016/j.chom.2019.01.014
620 Landa, K. J., Mossman, L. M., Whitaker, R. J., Rapti, Z., & Clifton, S. M. (2021). *Phage-antibiotic synergy*
621 *inhibited by temperate and chronic virus competition*. https://arxiv.org/abs/2104.08989v1
622 Leoni, L., Orsi, N., De Lorenzo, V., & Visca, P. (2000). Functional Analysis of PvdS, an Iron Starvation Sigma
623 Factor of *Pseudomonas aeruginosa*. *Journal of Bacteriology*, *182*(6), 1481–1491.
624 https://doi.org/10.1128/JB.182.6.1481-1491.2000
625 Little, J. W., Shepley, D. P., & Wert, D. W. (1999). Robustness of a gene regulatory circuit. *The EMBO Journal*,
626 *18*(15), 4299–4307. https://doi.org/10.1093/emboj/18.15.4299
627 Machanick, P., & Bailey, T. L. (2011). MEME-ChIP: Motif analysis of large DNA datasets. *Bioinformatics*, *27*(12),
628 1696–1697. https://doi.org/10.1093/bioinformatics/btr189
629 Makarova, K. S., Wolf, Y. I., Snir, S., & Koonin, E. V. (2011). Defense Islands in Bacterial and Archaeal Genomes
630 and Prediction of Novel Defense Systems. *Journal of Bacteriology*, *193*(21), 6039–6056.
631 https://doi.org/10.1128/JB.05535-11
632 Malek, A. A., Chen, C., Wargo, M. J., Beattie, G. A., & Hogan, D. A. (2011). Roles of Three Transporters,
633 CbcXWV, BetT1, and BetT3, in Pseudomonas aeruginosa Choline Uptake for Catabolism. *Journal of*
634 *Bacteriology*, *193*(12), 3033–3041. https://doi.org/10.1128/JB.00160-11
635 Malhotra, S., Hayes, D., & Wozniak, D. J. (2019). Cystic Fibrosis and Pseudomonas aeruginosa: The Host-
636 Microbe Interface. *Clinical Microbiology Reviews*, *32*(3), e00138-18.
637 https://doi.org/10.1128/CMR.00138-18
638 Markussen, T., Marvig, R. L., Gómez-Lozano, M., Aanæs, K., Burleigh, A. E., Høiby, N., Johansen, H. K., Molin, S.,
639 & Jelsbak, L. (2014). Environmental Heterogeneity Drives Within-Host Diversification and Evolution of
640 Pseudomonas aeruginosa. *mBio*, *5*(5). https://doi.org/10.1128/mBio.01592-14

641 Marshall, C. W., Gloag, E. S., Lim, C., Wozniak, D. J., & Cooper, V. S. (2021). Rampant prophage movement
642 among transient competitors drives rapid adaptation during infection. *Science Advances*, *7*(29),
643 eabh1489. https://doi.org/10.1126/sciadv.abh1489
644 Marvig, R. L., Sommer, L. M., Molin, S., & Johansen, H. K. (2015). Convergent evolution and adaptation of
645 Pseudomonas aeruginosa within patients with cystic fibrosis. *Nature Genetics*, *47*(1), 57–64.
646 https://doi.org/10.1038/ng.3148
647 McGrath, L. T., Mallon, P., Dowey, L., Silke, B., McClean, E., McDonnell, M., Devine, A., Copeland, S., & Elborn,
648 S. (1999). Oxidative stress during acute respiratory exacerbations in cystic fibrosis. *Thorax*, *54*(6), 518–
649 523. https://doi.org/10.1136/thx.54.6.518
650 Milne, I., Stephen, G., Bayer, M., Cock, P. J. A., Pritchard, L., Cardle, L., Shaw, P. D., & Marshall, D. (2013). Using
651 Tablet for visual exploration of second-generation sequencing data. *Briefings in Bioinformatics*, *14*(2),
652 193–202. https://doi.org/10.1093/bib/bbs012
653 Morgan, G. J., Hatfull, G. F., Casjens, S., & Hendrix, R. W. (2002). Bacteriophage Mu genome sequence:
654 Analysis and comparison with Mu-like prophages in Haemophilus, Neisseria and Deinococcus. *Journal
655 of Molecular Biology*, *317*(3), 337–359. https://doi.org/10.1006/jmbi.2002.5437
656 Nakagawa, I., Kurokawa, K., Yamashita, A., Nakata, M., Tomiyasu, Y., Okahashi, N., Kawabata, S., Yamazaki, K.,
657 Shiba, T., Yasunaga, T., Hayashi, H., Hattori, M., & Hamada, S. (2003). Genome Sequence of an M3
658 Strain of *Streptococcus pyogenes* Reveals a Large-Scale Genomic Rearrangement in Invasive Strains and
659 New Insights into Phage Evolution. *Genome Research*, *13*(6a), 1042–1055.
660 https://doi.org/10.1101/gr.1096703
661 Nanda, A. M., Thormann, K., & Frunzke, J. (2015). Impact of Spontaneous Prophage Induction on the Fitness of
662 Bacterial Populations and Host-Microbe Interactions. *Journal of Bacteriology*, *197*(3), 410–419.
663 https://doi.org/10.1128/JB.02230-14
664 Nguyen, A. T., O'Neill, M. J., Watts, A. M., Robson, C. L., Lamont, I. L., Wilks, A., & Oglesby-Sherrouse, A. G.
665 (2014). Adaptation of Iron Homeostasis Pathways by a Pseudomonas aeruginosa Pyoverdine Mutant in

666 the Cystic Fibrosis Lung. *Journal of Bacteriology*, *196*(12), 2265–2276.
667 https://doi.org/10.1128/JB.01491-14
668 O'Brien, S., Kümmerli, R., Paterson, S., Winstanley, C., & Brockhurst, M. A. (2019). Transposable temperate
669 phages promote the evolution of divergent social strategies in Pseudomonas aeruginosa populations.
670 *Proceedings of the Royal Society B: Biological Sciences*, *286*(1912), 20191794.
671 https://doi.org/10.1098/rspb.2019.1794
672 O'Brien, S., Williams, D., Fothergill, J. L., Paterson, S., Winstanley, C., & Brockhurst, M. A. (2017). High virulence
673 sub-populations in Pseudomonas aeruginosa long-term cystic fibrosis airway infections. *BMC*
674 *Microbiology*, *17*(1), 30. https://doi.org/10.1186/s12866-017-0941-6
675 Ojeniyi, B., Birch-Andersen, A., Mansa, B., Rosdahl, V. T., & HØIby, N. (1991). Morphology Of *Pseudomonas*
676 *aeruginosa* phages from the sputum of cystic fibrosis patients and from the phage typing set. *APMIS*,
677 *99*(7–12), 925–930. https://doi.org/10.1111/j.1699-0463.1991.tb01280.x
678 Oliver, A., Cantón, R., Campo, P., Baquero, F., & Blázquez, J. (2000). High Frequency of Hypermutable
679 Pseudomonas aeruginosa in Cystic Fibrosis Lung Infection. *Science*, *288*(5469), 1251–1253.
680 https://doi.org/10.1126/science.288.5469.1251
681 Owen, S. V., Wenner, N., Canals, R., Makumi, A., Hammarlöf, D. L., Gordon, M. A., Aertsen, A., Feasey, N. A., &
682 Hinton, J. C. D. (2017). Characterization of the Prophage Repertoire of African Salmonella Typhimurium
683 ST313 Reveals High Levels of Spontaneous Induction of Novel Phage BTP1. *Frontiers in Microbiology*, *8*.
684 https://doi.org/10.3389/fmicb.2017.00235
685 Perault, A. I., Chandler, C. E., Rasko, D. A., Ernst, R. K., Wolfgang, M. C., & Cotter, P. A. (2020). Host Adaptation
686 Predisposes Pseudomonas aeruginosa to Type VI Secretion System-Mediated Predation by the
687 Burkholderia cepacia Complex. *Cell Host & Microbe*, *28*(4), 534-547.e3.
688 https://doi.org/10.1016/j.chom.2020.06.019
689 R Core Team. (2023). *R: A Language and Environment for Statistical Computing* (4.3.1) [Computer software]. R
690 Foundation for Statistical Computing. https://www.R-project.org

691 Rau, M. H., Marvig, R. L., Ehrlich, G. D., Molin, S., & Jelsbak, L. (2012). Deletion and acquisition of genomic
692 content during early stage adaptation of Pseudomonas aeruginosa to a human host environment:
693 Bacterial genome reduction in human host. *Environmental Microbiology*, *14*(8), 2200–2211.
694 https://doi.org/10.1111/j.1462-2920.2012.02795.x
695 Robinson, J. T., Thorvaldsdóttir, H., Wenger, A. M., Zehir, A., & Mesirov, J. P. (2017). Variant Review with the
696 Integrative Genomics Viewer. *Cancer Research*, *77*(21), e31–e34. https://doi.org/10.1158/0008-
697 5472.CAN-17-0337
698 Robinson, L. A., Collins, A. C. Z., Murphy, R. A., Davies, J. C., & Allsopp, L. P. (2023). Diversity and prevalence of
699 type VI secretion system effectors in clinical Pseudomonas aeruginosa isolates. *Frontiers in*
700 *Microbiology*, *13*, 1042505. https://doi.org/10.3389/fmicb.2022.1042505
701 Rolain, J.-M., Francois, P., Hernandez, D., Bittar, F., Richet, H., Fournous, G., Mattenberger, Y., Bosdure, E.,
702 Stremler, N., Dubus, J.-C., Sarles, J., Reynaud-Gaubert, M., Boniface, S., Schrenzel, J., & Raoult, D.
703 (2009). Genomic analysis of an emerging multiresistant Staphylococcus aureus strain rapidly spreading
704 in cystic fibrosis patients revealed the presence of an antibiotic inducible bacteriophage. *Biology Direct*,
705 *4*(1), 1. https://doi.org/10.1186/1745-6150-4-1
706 Rollie, C., Chevallereau, A., Watson, B. N. J., Chyou, T., Fradet, O., McLeod, I., Fineran, P. C., Brown, C. M.,
707 Gandon, S., & Westra, E. R. (2020). Targeting of temperate phages drives loss of type I CRISPR–Cas
708 systems. *Nature*, *578*(7793), Article 7793. https://doi.org/10.1038/s41586-020-1936-2
709 Rossi, E., La Rosa, R., Bartell, J. A., Marvig, R. L., Haagensen, J. A. J., Sommer, L. M., Molin, S., & Johansen, H. K.
710 (2021). Pseudomonas aeruginosa adaptation and evolution in patients with cystic fibrosis. *Nature*
711 *Reviews Microbiology*, *19*(5), 331–342. https://doi.org/10.1038/s41579-020-00477-5
712 Schick, A., & Kassen, R. (2018). Rapid diversification of Pseudomonas aeruginosa in cystic fibrosis lung-like
713 conditions. *Proceedings of the National Academy of Sciences*, *115*(42), 10714–10719.
714 https://doi.org/10.1073/pnas.1721270115

715 Shah, M., Taylor, V. L., Bona, D., Tsao, Y., Stanley, S. Y., Pimentel-Elardo, S. M., McCallum, M., Bondy-Denomy,
716 J., Howell, P. L., Nodwell, J. R., Davidson, A. R., Moraes, T. F., & Maxwell, K. L. (2021). A phage-encoded
717 anti-activator inhibits quorum sensing in Pseudomonas aeruginosa. *Molecular Cell*, *81*(3), 571-583.e6.
718 https://doi.org/10.1016/j.molcel.2020.12.011
719 Stribling, W., Hall, L. R., Powell, A., Harless, C., Martin, M. J., Corey, B. W., Snesrud, E., Ong, A., Maybank, R.,
720 Stam, J., Bartlett, K., Jones, B. T., Preston, L. N., Lane, K. F., Thompson, B., Young, L. M., Kwak, Y. I.,
721 Barsoumian, A. E., Markelz, A.-E., … Lebreton, F. (2023). *Detecting, mapping, and suppressing the*
722 *spread of a decade-long* Pseudomonas aeruginosa *nosocomial outbreak with genomics* [Preprint].
723 Microbiology. https://doi.org/10.1101/2023.07.24.550326
724 Tai, A. S., Sherrard, L. J., Kidd, T. J., Ramsay, K. A., Buckley, C., Syrmis, M., Grimwood, K., Bell, S. C., & Whiley, D.
725 M. (2017). Antibiotic perturbation of mixed-strain Pseudomonas aeruginosa infection in patients with
726 cystic fibrosis. *BMC Pulmonary Medicine*, *17*. https://doi.org/10.1186/s12890-017-0482-7
727 Tariq, M. A., Everest, F. L. C., Cowley, L. A., De Soyza, A., Holt, G. S., Bridge, S. H., Perry, A., Perry, J. D., Bourke,
728 S. J., Cummings, S. P., Lanyon, C. V., Barr, J. J., & Smith, D. L. (2015). A metagenomic approach to
729 characterize temperate bacteriophage populations from Cystic Fibrosis and non-Cystic Fibrosis
730 bronchiectasis patients. *Frontiers in Microbiology*, *6*. https://doi.org/10.3389/fmicb.2015.00097
731 Tariq, M. A., Everest, F. L. C., Cowley, L. A., Wright, R., Holt, G. S., Ingram, H., Duignan, L. A. M., Nelson, A.,
732 Lanyon, C. V., Perry, A., Perry, J. D., Bourke, S., Brockhurst, M. A., Bridge, S. H., Soyza, A. D., & Smith, D.
733 L. (2019). Temperate Bacteriophages from Chronic Pseudomonas aeruginosa Lung Infections Show
734 Disease-Specific Changes in Host Range and Modulate Antimicrobial Susceptibility. *mSystems*, *4*(4).
735 https://doi.org/10.1128/mSystems.00191-18
736 Toussaint, A., & Rice, P. A. (2017). Transposable phages, DNA reorganization and transfer. *Current Opinion in*
737 *Microbiology*, *38*, 88–94. https://doi.org/10.1016/j.mib.2017.04.009

Vaca-Pacheco, S., Paniagua-Contreras, G. L., García-González, O., & de la Garza, M. (1999). The Clinically Isolated FIZ15 Bacteriophage Causes Lysogenic Conversion in Pseudomonas aeruginosa PAO1. *Current Microbiology*, *38*(4), 239–243. https://doi.org/10.1007/PL00006794

Vanderwoude, J., Azimi, S., Read, T., & Diggle, S. P. (2023). *Unraveling Genomic Diversity in Pseudomonas aeruginosa Cystic Fibrosis Lung Infection and Its Impact on Antimicrobial Resistance* [Preprint]. Microbiology. https://doi.org/10.1101/2023.06.14.544983

Vergnaud, G., Midoux, C., Blouin, Y., Bourkaltseva, M., Krylov, V., & Pourcel, C. (2018). Transposition Behavior Revealed by High-Resolution Description of Pseudomonas Aeruginosa Saltovirus Integration Sites. *Viruses*, *10*(5), Article 5. https://doi.org/10.3390/v10050245

Vorontsova, D., Datsenko, K. A., Medvedeva, S., Bondy-Denomy, J., Savitskaya, E. E., Pougach, K., Logacheva, M., Wiedenheft, B., Davidson, A. R., Severinov, K., & Semenova, E. (2015). Foreign DNA acquisition by the I-F CRISPR–Cas system requires all components of the interference machinery. *Nucleic Acids Research*, *43*(22), 10848–10860. https://doi.org/10.1093/nar/gkv1261

Walker, D. M., Freddolino, P. L., & Harshey, R. M. (2020). A Well-Mixed E. coli Genome: Widespread Contacts Revealed by Tracking Mu Transposition. *Cell*, *180*(4), 703-716.e18. https://doi.org/10.1016/j.cell.2020.01.031

Walker, D. M., & Harshey, R. M. (2020). Deep sequencing reveals new roles for MuB in transposition immunity and target-capture, and redefines the insular Ter region of E. coli. *Mobile DNA*, *11*(1), 26. https://doi.org/10.1186/s13100-020-00217-9

Watson, B. N. J., Pursey, E., Gandon, S., & Westra, E. R. (2023). Transient eco-evolutionary dynamics early in a phage epidemic have strong and lasting impact on the long-term evolution of bacterial defences. *PLOS Biology*, *21*(9), e3002122. https://doi.org/10.1371/journal.pbio.3002122

Weitz, J. S., Li, G., Gulbudak, H., Cortez, M. H., & Whitaker, R. J. (2019). Viral invasion fitness across a continuum from lysis to latency. *Virus Evolution*, *5*(1). https://doi.org/10.1093/ve/vez006

762 Wickham, H., Averick, M., Bryan, J., Chang, W., McGowan, L., François, R., Grolemund, G., Hayes, A., Henry, L.,
763 Hester, J., Kuhn, M., Pedersen, T., Miller, E., Bache, S., Müller, K., Ooms, J., Robinson, D., Seidel, D.,
764 Spinu, V., … Yutani, H. (2019). Welcome to the Tidyverse. *Journal of Open Source Software*, *4*(43), 1686.
765 https://doi.org/10.21105/joss.01686
766 Willner, D., Haynes, M. R., Furlan, M., Hanson, N., Kirby, B., Lim, Y. W., Rainey, P. B., Schmieder, R., Youle, M.,
767 Conrad, D., & Rohwer, F. (2012). Case Studies of the Spatial Heterogeneity of DNA Viruses in the Cystic
768 Fibrosis Lung. *American Journal of Respiratory Cell and Molecular Biology*, *46*(2), 127–131.
769 https://doi.org/10.1165/rcmb.2011-0253OC
770 Winstanley, C., O'Brien, S., & Brockhurst, M. A. (2016). Pseudomonas aeruginosa Evolutionary Adaptation and
771 Diversification in Cystic Fibrosis Chronic Lung Infections. *Trends in Microbiology*, *24*(5), 327–337.
772 https://doi.org/10.1016/j.tim.2016.01.008
773 Workentine, M. L., Sibley, C. D., Glezerson, B., Purighalla, S., Norgaard-Gron, J. C., Parkins, M. D., Rabin, H. R.,
774 & Surette, M. G. (2013). Phenotypic Heterogeneity of Pseudomonas aeruginosa Populations in a Cystic
775 Fibrosis Patient. *PLoS ONE*, *8*(4), e60225. https://doi.org/10.1371/journal.pone.0060225
776 Zegans, M. E., Wagner, J. C., Cady, K. C., Murphy, D. M., Hammond, J. H., & O'Toole, G. A. (2009). Interaction
777 between Bacteriophage DMS3 and Host CRISPR Region Inhibits Group Behaviors of Pseudomonas
778 aeruginosa. *Journal of Bacteriology*, *191*(1), 210–219. https://doi.org/10.1128/JB.00797-08
779 Zhang, M., Hao, Y., Yi, Y., Liu, S., Sun, Q., Tan, X., Tang, S., Xiao, X., & Jian, H. (2023). Unexplored diversity and
780 ecological functions of transposable phages. *The ISME Journal*. https://doi.org/10.1038/s41396-023-
781 01414-z
782 Zong, C., So, L., Sepúlveda, L. A., Skinner, S. O., & Golding, I. (2010). Lysogen stability is determined by the
783 frequency of activity bursts from the fate-determining gene. *Molecular Systems Biology*, *6*(1), 440.
784 https://doi.org/10.1038/msb.2010.96
785
786

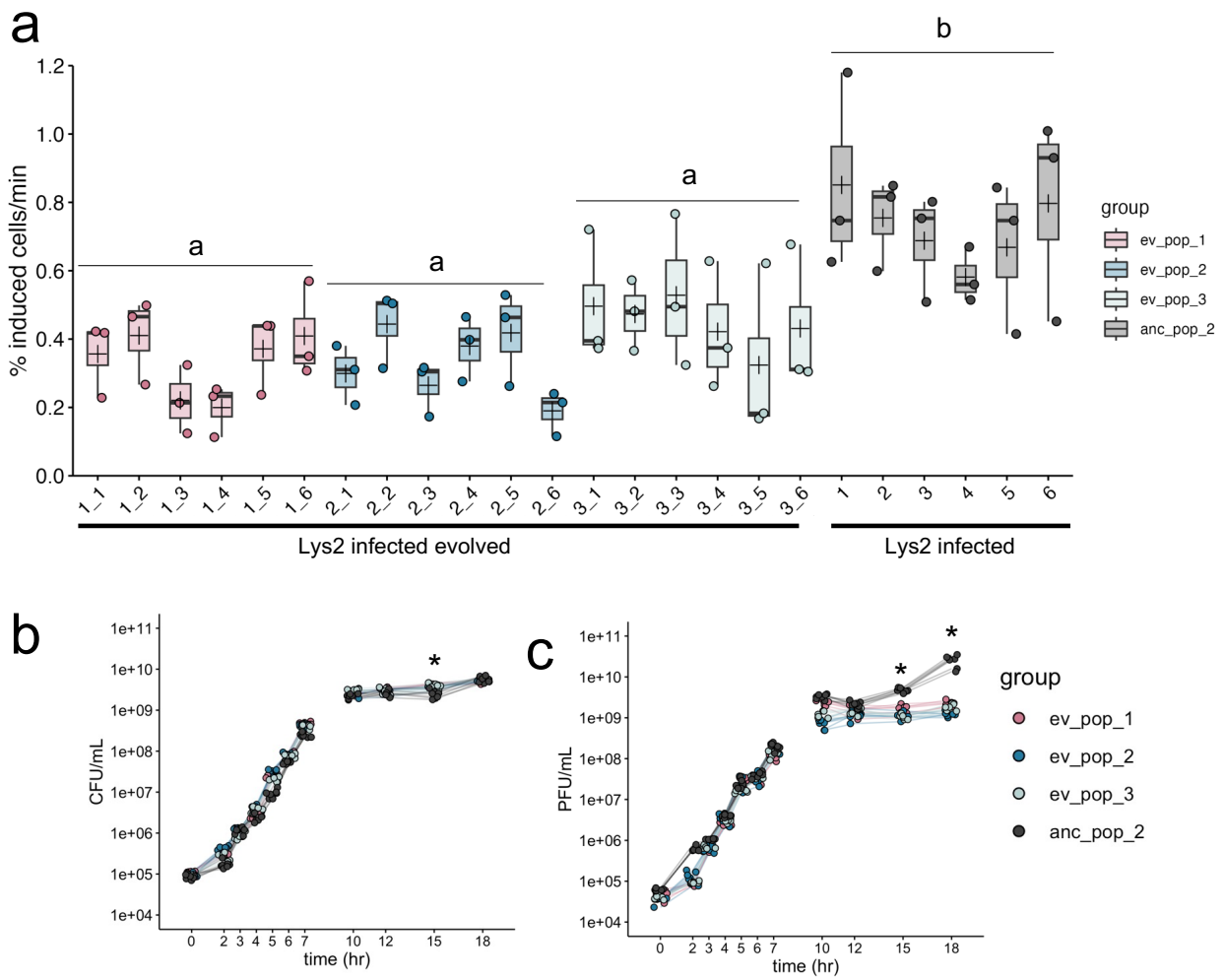

Figure 1. Experimental evolution results in lowered lysogen spontaneous induction. A) Spontaneous induction was measured in exponential phase in six individual isolates from each of three evolved lysogen replicates (ev_pop_1, pink), (ev_pop_2, blue), (ev_pop_3, light blue) and the ancestral strain Lys2 (anc_pop_2, grey). Points are the means of three technical replicates. Bars in the boxplots represent the median; crosses represent the means. Upper and lower bounds of the box are the upper and lower interquartile ranges. Significance was tested with an ANOVA ($F_{3,68}$ = 23.27, p-value = 1.78e-10). Letters indicate significance; groups with different letters have a p-value <0.05; groups with the same or overlapping letters have a p-value of >0.05. B) Bacterial growth curve of all isolates through 18 hours, measured by CFU. C) PFUs sampled through growth curve of all isolates (except the non-lysogenic WT PA14). In B) and C), stationary phase was measured in separate experiments, as indicated by the line breaks between 7 and 10 hours. Points represent the mean of three biological replicates. Asterisks represent a significant difference between the ancestral and evolved populations. Significance was calculated with a Mann-Whitney U test per time point.

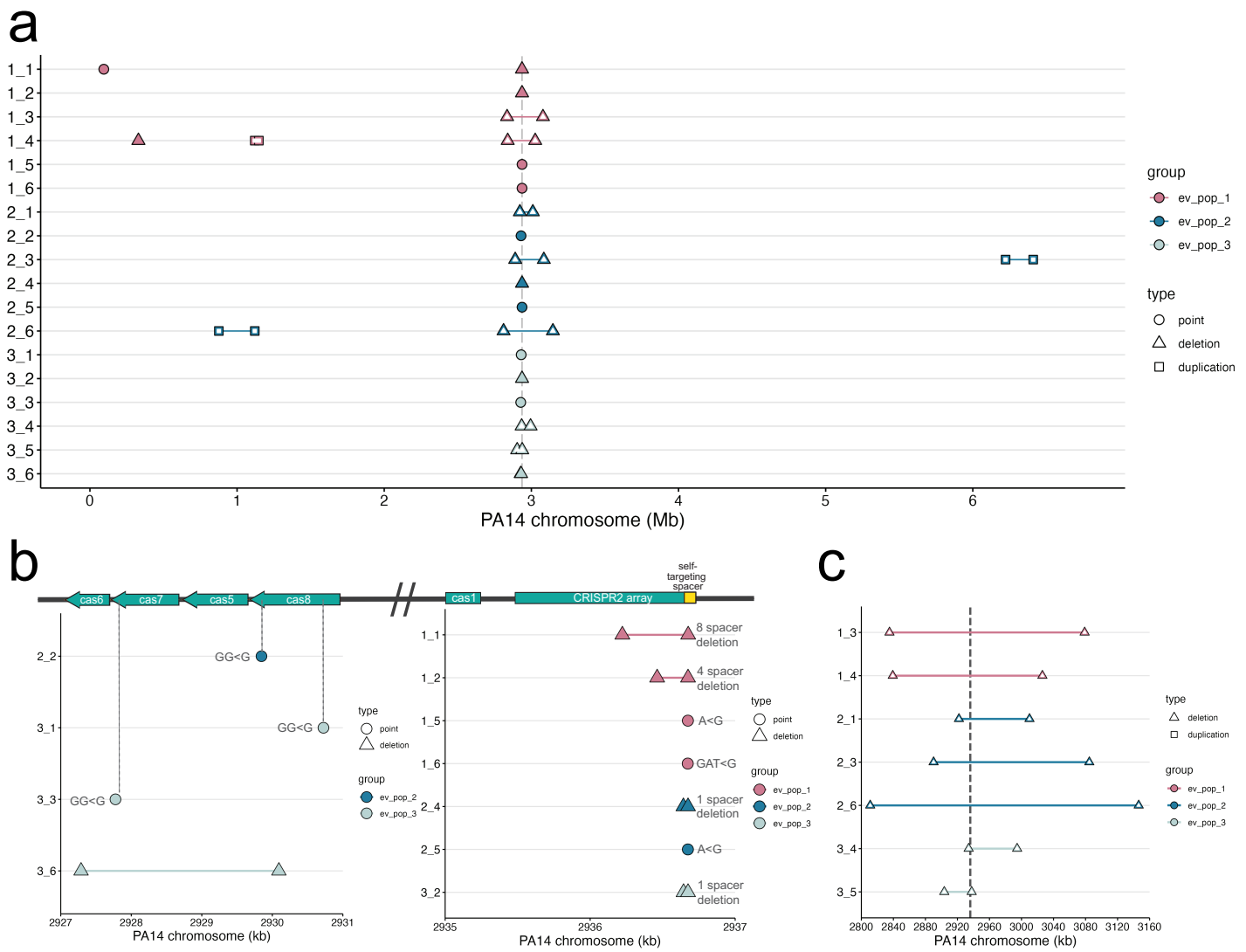

Figure 2. Mutations in infected evolved strains are distinct from uninfected evolved strains. A) Graph of mutations found in all infected evolved samples. B) Close-up of point mutations and small deletions in infected evolved strains. The majority are found in the self-targeting spacer 1 in the 2nd CRISPR array. Gray dashed lines indicate location in the genes. C) Close-up of large deletions in infected evolved strains. Gray dashed double lines indicate the boundaries of the CRISPR-Cas region. In A-C), the y-axis indicates sample ID; x-axis indicates position on the PA14 reference chromosome. Points represent point mutations; triangles spanned by a segment represent deletions of the spanned region; squares spanned by a segment represent duplications of the spanned region. White fill indicates a mutation that was caused by a virus.

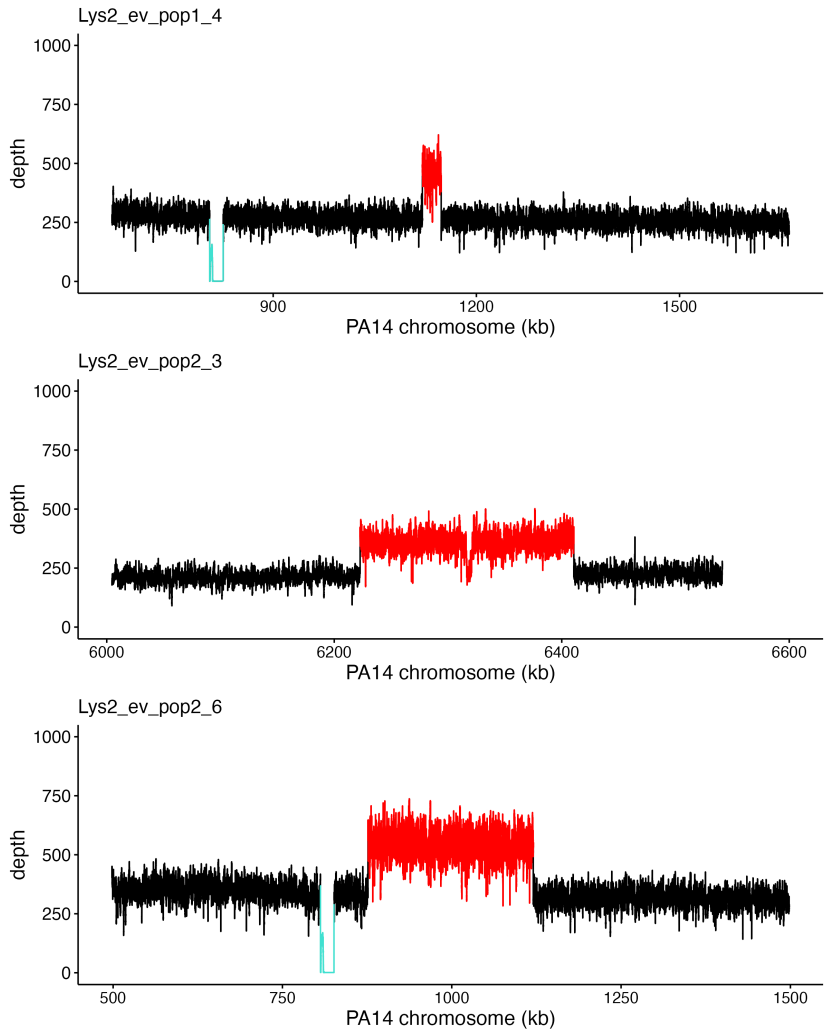

Figure 3. Location and coverage of large duplicated regions in three evolved lysogens. Area between viral insertion sites has higher coverage than the rest of the genome. X-axis is position on the PA14 chromosome. Y-axis is depth of sequencing coverage at that nucleotide. Red line represents the region in between two viral insertion sites. Cyan line is ancestral insertion site (where applicable). Black line is 500,000 randomly subsampled positions across the genome.

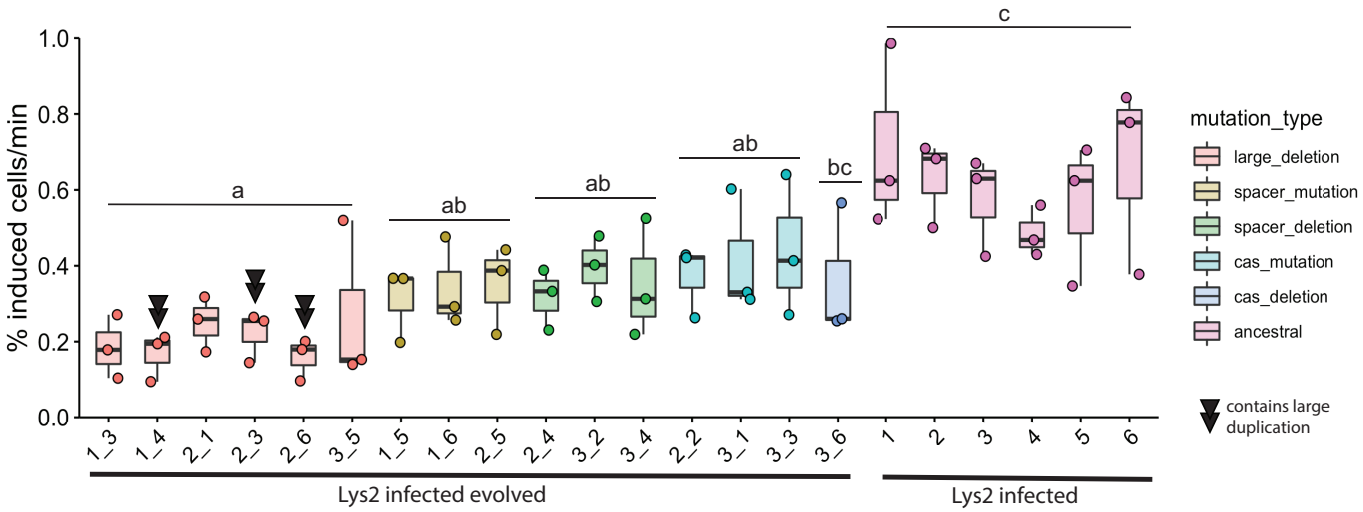

Figure 4. Genomic variation may explain phenotypic variation. Evolved isolates were grouped by type of mutation. Colors of points and boxes represent groups. Points are means of experimental replicates. Box plots are as in Figure 1. Isolates with double black triangles have large duplications which are due to another viral insertion. Significance was determined with an ANOVA with Tukey adjustment using the log-transformed values ($F_{5,66}$ = 19.3, p-value = 8.725e-12). Letters indicate significance; groups with different letters have a p-value <0.05 between them; groups with the same or overlapping letters have a p-value of >0.05 between them.

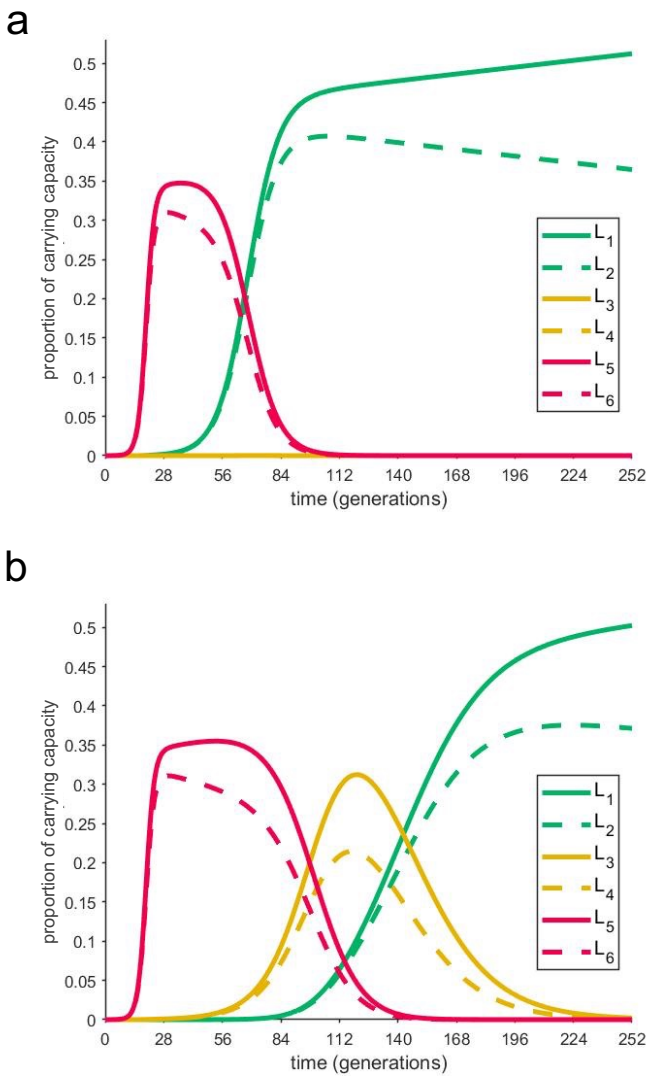

Figure 5. Coexistence of different rates of spontaneous induction depends on the order of their introduction. A mathematical model describes the behavior of several lysogens with different spontaneous induction values. These graphs describe the growth of six lysogens over time in one continuously growing culture. The y-axis represents the proportion of carrying capacity of the medium; the x-axis is time in PA14 generations. Each lysogen was assigned a spontaneous induction value from the experimentally determined range. Each pair (L1/L2; L3/L4; L5/L6) in a certain range are taken from values in the same group, from lowest to highest spontaneous induction values (L1 is the lowest; L6 is the highest). In A) the highest spontaneous inducers are introduced first. At approximately 9 hours, low inducers are introduced; after about 1 day, medium inducers are introduced and do not establish. In B) the highest spontaneous inducers are introduced first. At approximately 9 hours, medium inducers are introduced; after about 1 day, low inducers are introduced and establish, resulting in a period of coexistence between medium and low inducers that is observed experimentally.

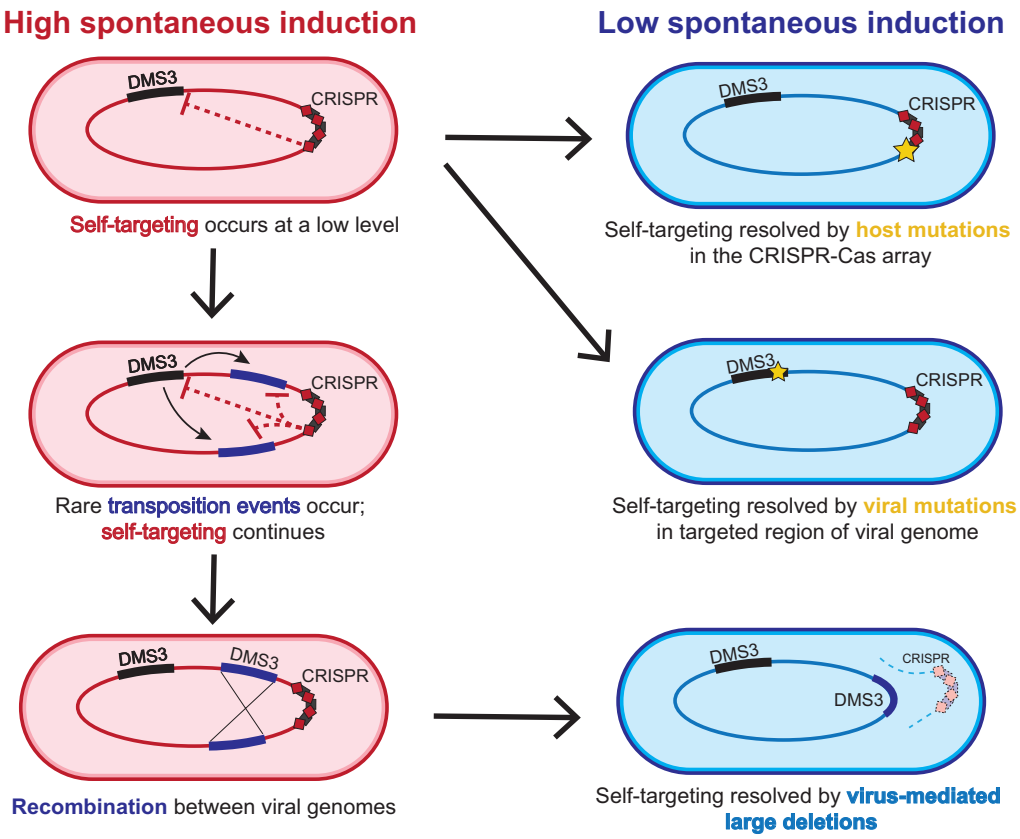

Figure 6. Model of self-targeting leading to DMS3 transposition around the genome. Spontaneous induction caused by CRISPR self-targeting is resolved in two modes. Cells with high spontaneous induction are indicated in the first column, in red. One mode, in the first column, relies on low levels of DMS3 escape from lysogenic repression which result in rare transposition events around the genome. Recombination between multiple DMS3 chromosomes leads to large deletions, which may include the CRISPR area and result in cells with lower spontaneous induction (blue). In the second mode, self-targeting may be resolved by host mutations in the CRISPR-Cas region, or by viral mutations in the targeted region (not recovered in this study).

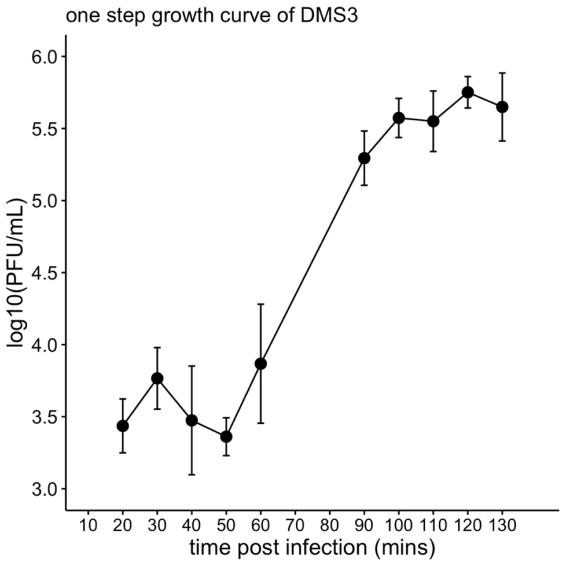

849

850 **Figure S1. One step growth curve of DMS3**. Points represent the mean of experimental replicates (n=6 for
851 all other time points except 20 mins (n=3) and 100 mins (n = 2). Error bars represent standard deviation. The
852 x-axis is time post-infection in minutes; the y-axis is the $\log_{10}$ of PFU/mL. Plateau 1 is the average of all values
853 from 20-50 minutes; Plateau 2 is the average of all values from 100-130 minutes.

854

855

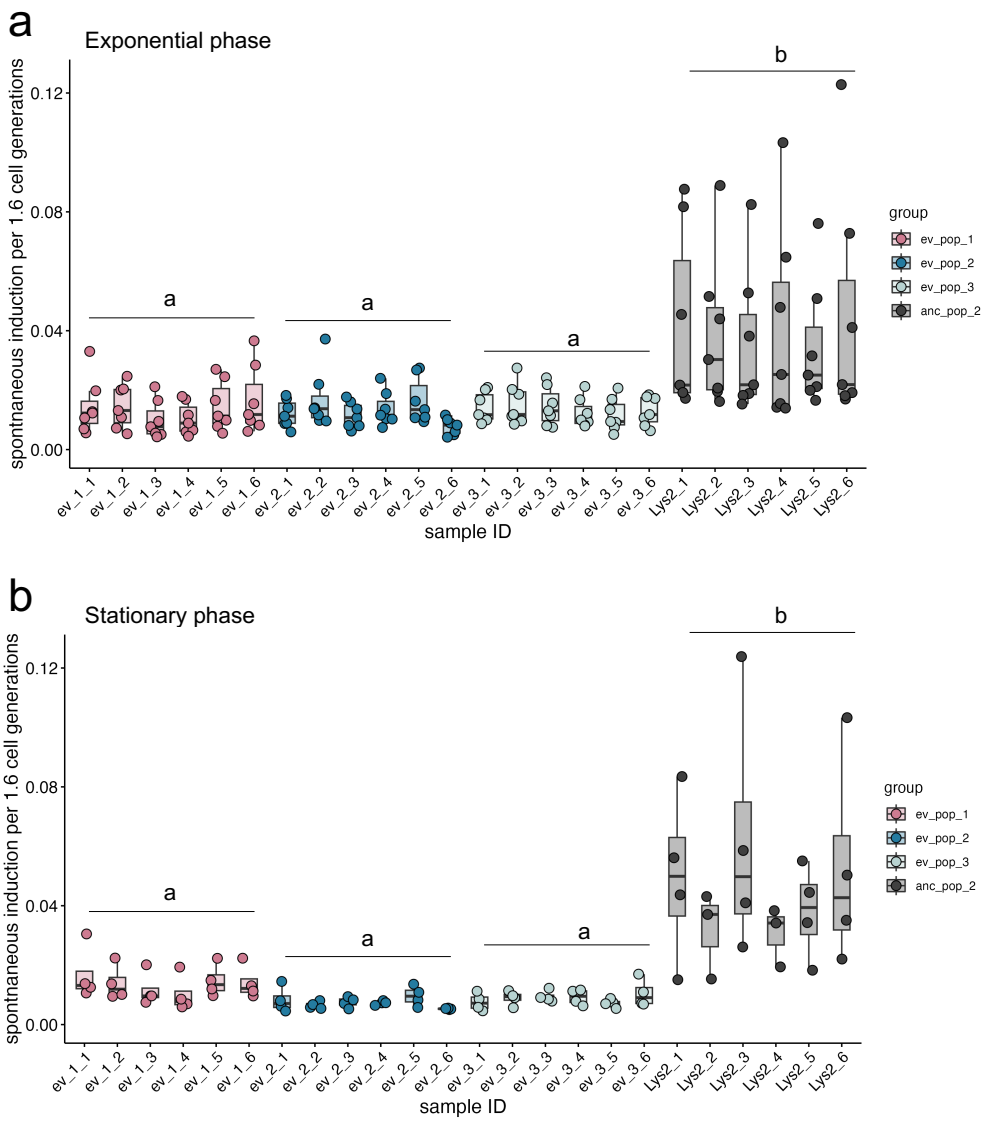

856

857 **Figure S2. Spontaneous induction calculated with Zong et al formula.** A) Spontaneous induction in
858 exponential phase. X-axis is time in hours; y-axis is spontaneous induction per hour, or 1.6 cell generations of
859 PA14. B) Spontaneous induction in stationary phase. X-axis is sample ID; y-axis is spontaneous induction per
860 hour. Significance was calculated as the spontaneous induction value as a function of group with Dunn's Test
861 of Multiple Comparisons and Bonferroni correction. Letters indicate significance; groups with different letters
862 have a p-value <0.05 between them; groups with the same or overlapping letters have a p-value of >0.05
863 between them.

864

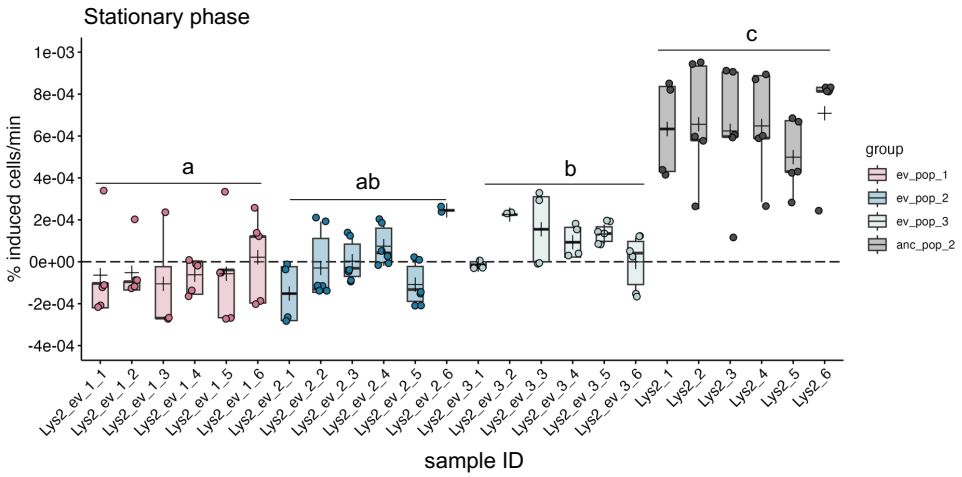

Figure S3. Experimental evolution results in lowered lysogen spontaneous induction in stationary phase. Spontaneous induction was measured in stationary phase. Six individual isolates from each of three lysogen replicates (ev_pop_1, pink), (ev_pop_2, blue), (ev_pop_3, light blue) and the ancestral strain Lys2 (anc_pop_2, grey) were measured. Points are the means of one experimental replicate from three technical replicates. Boxplots are as in Figure 1. Significance was tested with an ANOVA ($F_{3,109}$ = 86.98, P < 2.2e-16). Letters indicate significance; groups with different letters have a p-value <0.05; groups with the same or overlapping letters have a p-value of > 0.05.

Figure S4. DMS3 is partially matched by CRISPR spacers in PA14 and is resolved by host mutations. Map of spacer-protospacer match compared to escape mutations in the host spacer that evolved in two single isolates in parallel cultures. Five mismatched bases on the virus are highlighted in bold red font and lack lines indicating base pairing; escape mutations are highlighted in blue and lack lines indicating base pairing. Hyphens indicate a deletion of those bases.

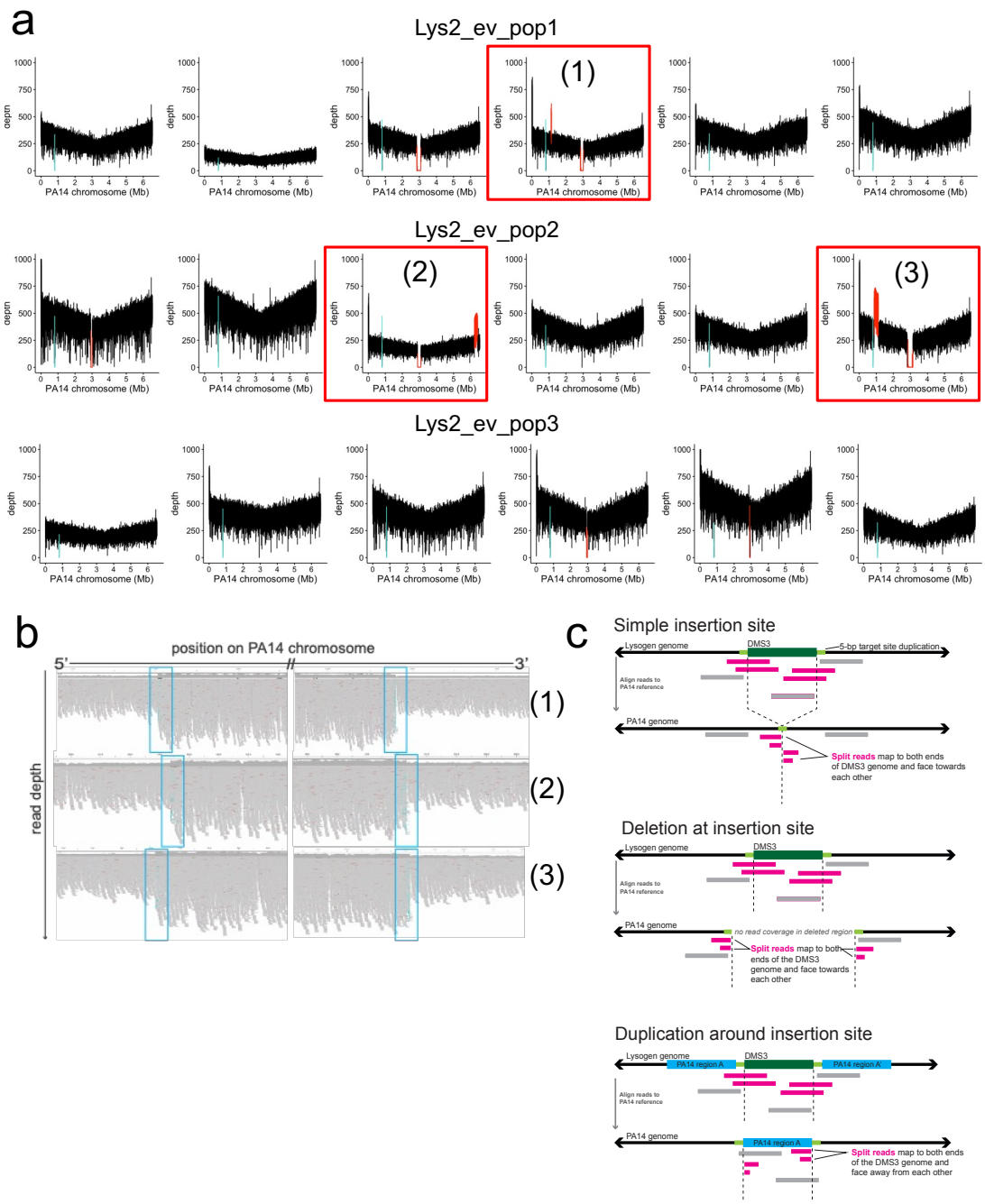

Figure S5. Analysis of duplicated regions. A) Representative coverage across the chromosome for each evolved isolate. Ancestral Lys2 insertion site with intervening deletion is shown in cyan. Regions of double coverage bounded by DMS3 insertion sites are shown in red. 500,000 positions across the genome were randomly subsampled. Some peaks of coverage towards the far end are in an unannotated, repetitive region upstream of TSCPD-domain containing protein. B) IGV view of mapped reads at the insertion site boundaries and coverage changes. All graphs are 5' to 3'; note the location of cyan reads facing out from the area of higher coverage, and away from the other overlap. C) Schematic of how transposable phages appear in short read data.

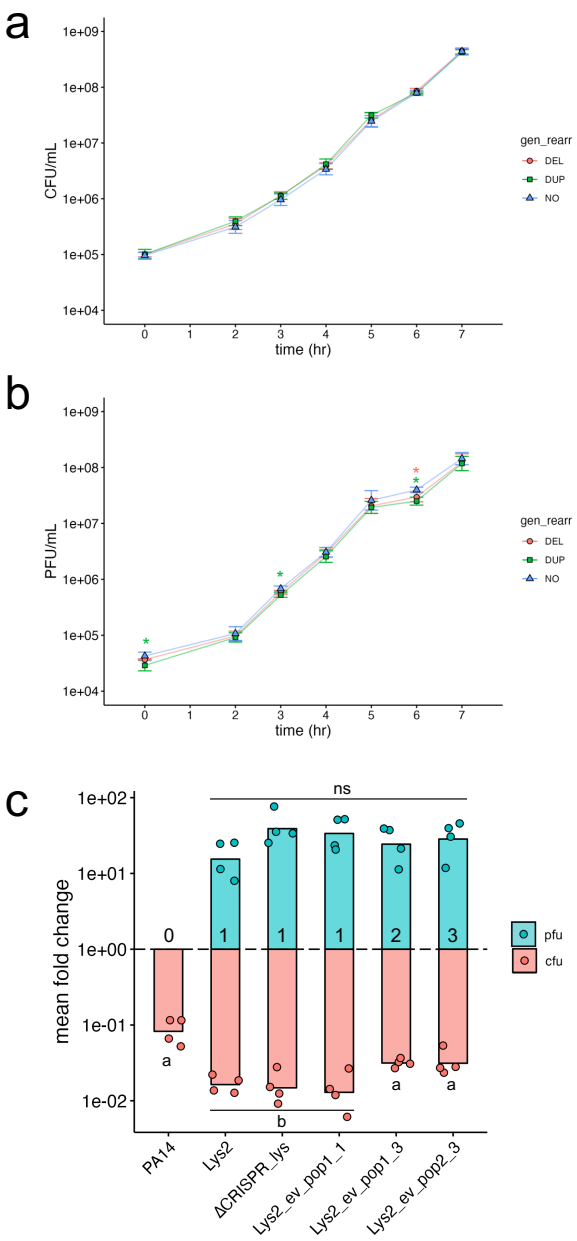

Figure S6. Genome rearrangements are tolerated without growth defects in rich medium in evolved lysogens. A) CFUs and B) PFUs of evolved lysogens in exponential growth. Time is indicated on the x-axis in hours, and CFUs or PFUs are indicated on the y-axis. Asterisks indicate significant differences by Dunn's test between the genomic rearrangement ("DEL": deletion; "DUP": duplication) indicated by the color, and the "NO" genomic rearrangement group (the average of all other lysogens). C) Induction of lysogens with increasing numbers of viral genomes. Numbers in the PFU column represent how many viral genomes are present in the lysogen. Dunn's Test of Multiple Comparisons with a Bonferroni correction was used to test the interaction between the mean fold change and the number of phages present. Points represent the mean of one experimental replicate (three technical replicates each). Bars represent the mean of all experimental replicates. Letters indicate statistical significance between groups; groups with the same letter are not statistically significant. "NS" = not significant.

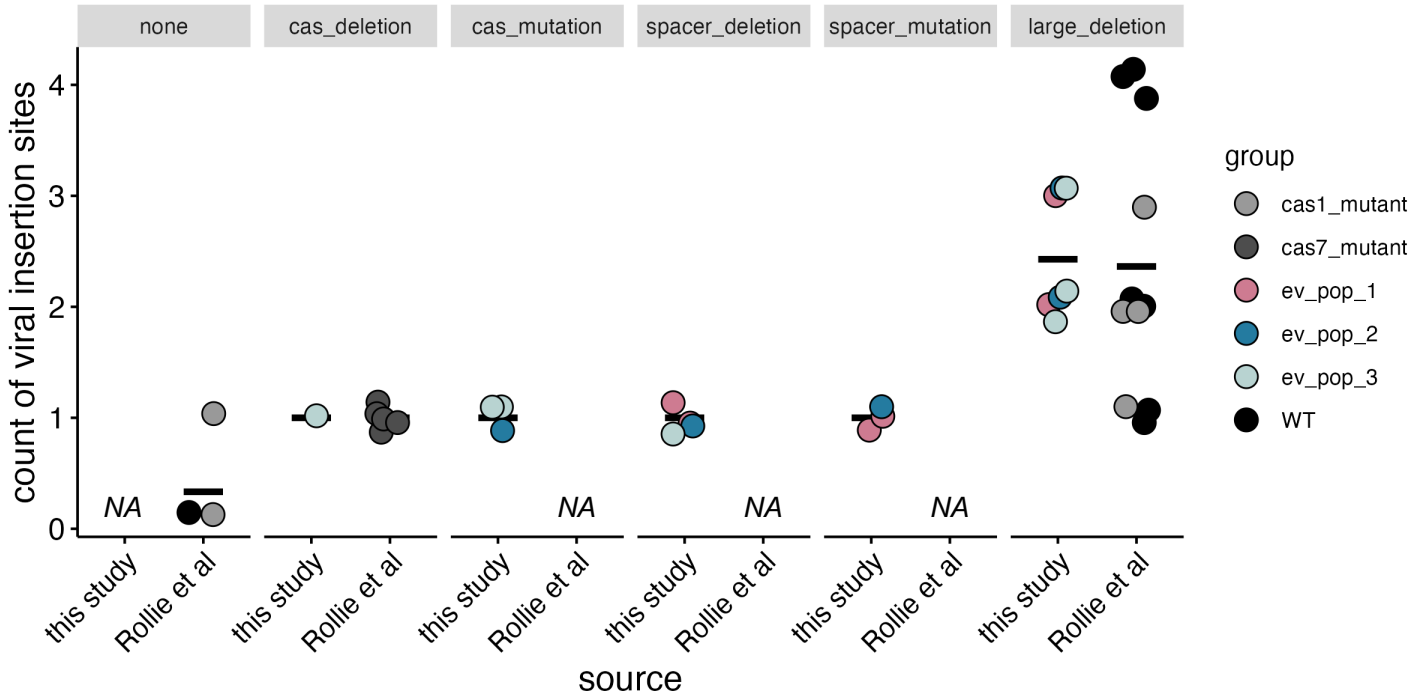

Fig S7. Polylysogeny does not arise in the absence of self-targeting. Y-axis describes the number of viral insertion sites recovered from each isolate; X-axis describes the source of the isolates (either this study or Rollie et al) and is broken up by the type of mutation which the isolate is classified by. Black bars indicate the mean. Points represent one isolate. Point color indicates either what replicate it came from (as in this study) or in what strain background the evolution experiment was started (in Rollie et al). NA: no isolates were recovered in that mutation type category.

Strain	Description	Source
PA14	WT P. aeruginosa strain	George O'Toole
Lys2	PA14(DMS3) lysogen	Zegans et al, 2009
PA14ΔCRISPR	CRISPR deletion	Cady et al, 2011
PA14ΔCRISPR(DMS3)	CRISPR deletion lysogen	Cady et al, 2011
PA14Δpyocin	ΔR/F pyocin operon (PA14_07970 – PA14_08330)	Heussler et al, 2016
PA14Δpyocin(DMS3)_1	ΔR/F pyocin operon DMS3 lysogen	This study
PA14Δpyocin(DMS3)_2	ΔR/F pyocin operon DMS3 lysogen	This study
PA14Δpyocin(DMS3)_3	ΔR/F pyocin operon DMS3 lysogen	This study

914

915 **Table S1. List of strains used in this study.**

Lys2 Deletion Boundaries: 806165-826108 on PA14 Reference Genome		
Gene no. (5'-3')	**Deleted gene**	**Description**
1	PhzG	phenazine biosynthesis FMN-dependent oxidase
2	PhzF	phenazine biosynthesis protein; trans-2,3-dihydro-3-hydroxyanthranilate isomerase
3	PhzE	phenazine biosynthesis protein
4	PhzD	phenazine biosynthesis protein
5	PhzC	phenazine biosynthesis protein; phospho-2-dehydro-3-deoxyheptonate aldolase
6	PhzB	phenazine biosynthesis protein
7	PhzA	phenazine biosynthesis protein;
8	PhzM	phenazine-1-carboxylate N-methyltransferase
9	OpmD	multidrug efflux transporter outer membrane subunit; TolC family protein
10	MexI	MexW/MexI family multidrug efflux RND transporter permease subunit
11	MexH	MexH family multidrug efflux RND transporter periplasmic adaptor subunit
12	MexG	DoxX family protein; multidrug efflux RND transporter inhibitory subunit
13	PpgL	Gluconolactonase; 3-carboxymuconate cyclase
14	NmoR	LysR family transcriptional regulator
15	NmoA	nitronate monooxygenase
16	-	D-alanine--D-alanine ligase
17	-	MBL fold metallo-hydrolase

916

917 **Table S2. Genes contained in Lys2 deletion.** All functional predictions were confirmed by BLASTX using the
918 protein RefSeq database.

919

Supplemental Information

The following parameter values were used in the model equations:

$$\frac{dL_i}{dt} = rL_i\left(1 - \sum_{j=1}^{6}\left(L_j + I_j\right)\right) - q_i L_i$$

$$\frac{dI_i}{dt} = -\delta I_i + q_i L_i$$

$$\frac{dV_i}{dt} = \beta\delta I_i - \mu V_i.$$

$$q_1 = 0.1, q_2 = 0.102, q_3 = 0.17, q_4 = 0.175, q_5 = 0.288, q_6 = 0.293$$

and

$$r = 1, \beta = 45, \delta = 4, \mu = 1.$$

Each generation lasts 38 minutes. The initial conditions used were $\frac{1}{6} \times 10^{-4}$ for each L_i, which was added at the prescribed times. I_i and V_i were initially zero for each $i = 1, \ldots, 6$.